6 The Physics of Doped Mott Insulators

Robert Eder
Institute for Quantum Materials and Technologies
Karlsruhe Institute of Technology

Contents

E. Pavarini and E. Koch (eds.)
Topology, Entanglement, and Strong Correlations
Modeling and Simulation Vol. 10
Forschungszentrum Jülich, 2020, ISBN 978-3-95806-466-9
http://www.cond-mat.de/events/correl20

1 Introduction

Following the discovery of copper oxide superconductors with their spectacularly high superconducting transition temperatures by Bednorz and Müller [1], the problem of the doped Mott insulator has become a central issue in solid state physics. Still, after more than 30 years of research and thousands of papers devoted to this subject, there is no generally accepted theory for this problem. So what exactly do we mean by 'doped Mott insulator' and why is this problem so hard to solve?

Let us consider a two-dimensional square lattice with lattice constant $a = 1$, which consists of $N = L^2$ sites and impose periodic boundary conditions with period L along both the x- and y-direction. We denote the number of electrons with spin σ by N_σ, the total number of electrons by $N_e = N_\uparrow + N_\downarrow$. Also, we denote densities per site by n, for example $n_e = N_e/N$. To explain the idea of a Mott-insulator it would be neither necessary that the system is two-dimensional, nor that we have a square lattice, but this is the suitable geometry to describe the CuO_2 planes in copper oxide superconductors. We assume that there is one s-like atomic orbital $|\phi_i\rangle$ centered at each lattice site i. Orbitals on different sites are assumed to be orthogonal, $\langle\phi_i|\phi_j\rangle = \delta_{i,j}$, but there may be nonvanishing matrix elements of the Hamiltonian – that means the kinetic and potential energy – between them, $\langle\phi_i|H|\phi_j\rangle = -t_{i,j}$. We assume that the orbital $|\phi\rangle$ is the same for each lattice site, whence the matrix element $\langle\phi_i|\phi_j\rangle$ depends only on the distance between i and j: $t_{i,j} = t_{\mathbf{R}_i - \mathbf{R}_j}$. We also assume that the atomic orbital $|\phi_i\rangle$ decays exponentially, $\langle\mathbf{r}|\phi_i\rangle \propto e^{-|\mathbf{r}-\mathbf{R}_i|/\zeta}$, so we expect $t_{\mathbf{R}} \propto e^{-|\mathbf{R}|/\zeta}$ and $t_{i,j}$ will differ appreciably from zero only for close neighbors. Introducing operators $c^\dagger_{i,\sigma}$ which create an electron of z-spin σ in orbital $|\phi_i\rangle$ the Hamiltonian reads

$$H_0 = -\sum_{i,j} t_{i,j} \sum_\sigma c^\dagger_{i,\sigma} c_{j,\sigma} = \sum_{\mathbf{k}} \sum_\sigma \varepsilon_{\mathbf{k}}\, c^\dagger_{\mathbf{k},\sigma} c_{\mathbf{k},\sigma}.$$

The second expression for H_0 is obtained by Fourier transformation

$$c^\dagger_{\mathbf{k},\sigma} = \frac{1}{\sqrt{N}} \sum_j e^{i\mathbf{k}\cdot\mathbf{R}_j}\, c^\dagger_{j,\sigma} \quad\Rightarrow\quad \varepsilon_{\mathbf{k}} = -\frac{1}{N}\sum_{i,j} t_{i,j}\, e^{i\mathbf{k}\cdot(\mathbf{R}_i - \mathbf{R}_j)} = -\sum_{\mathbf{R}} t_{\mathbf{R}}\, e^{i\mathbf{k}\cdot\mathbf{R}}. \tag{1}$$

Here $\mathbf{k} = \left(\frac{2n\pi}{L}, \frac{2m\pi}{L}\right)$ with $-L/2 < m, n \le L/2$ is a wave vector in the first Brillouin zone. Unless otherwise stated we will from now on assume that $t_{i,j}$ is different from zero only for nearest neighbors i and j and denote its value by t, whence $\varepsilon_{\mathbf{k}} = -2t\big(\cos(k_x) + \cos(k_y)\big)$. The number of wave vectors $\mathbf{k}$ equals N and the ground state for N electrons is obtained by 'filling the band from below', that means occupying those $N/2$ wave vectors $\mathbf{k}$ which minimize the sum $\sum_{\mathbf{k}} \varepsilon_{\mathbf{k}}$ with two electrons of opposite spin. The band therefore is half-filled, the Fermi surface covers precisely half of the Brillouin zone and we have a metal.

In the discussion so far we have ignored the Coulomb interaction between the electrons. Recalling that the atomic orbital $\langle\mathbf{r}|\phi_i\rangle \propto e^{-|\mathbf{r}-\mathbf{R}_i|/\zeta}$, we expect that if the orbital is occupied by two electrons of opposite spin, the electrostatic energy is $U \propto e^2/\zeta$, whereas it is $\propto e^2/a$ if the electrons are in orbitals on different sites. If we take the limit of a 'small atomic orbital',

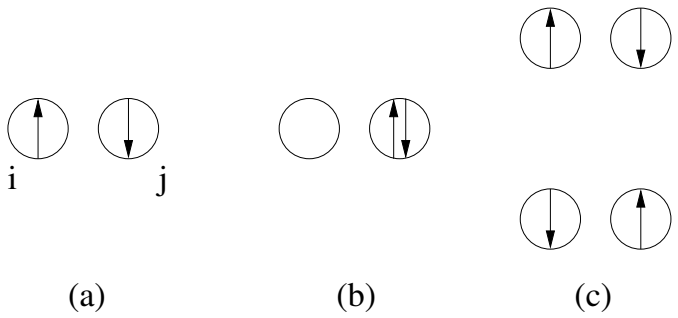

Fig. 1: *An exchange process in a Mott insulator.*

$\zeta \to 0$, we find $U/t \to \infty$ – accordingly we neglect the Coulomb repulsion $\propto e^2/a$ between electrons in different orbitals. Taking the extreme limit $U/t = \infty$ and returning to the problem of finding the ground state with N electrons we find that there is precisely one electron in each of the N orbitals (putting two electrons into the same orbital increases the energy by the large amount U). The electrons thus are 'frozen in' and cannot react to an applied electric field, so that the system is an insulator. This is the prototype of a *Mott insulator*: a system which would be a metal in the band picture, but is an insulator due to the strong Coulomb repulsion between electrons in 'small' atomic orbitals. It should be noted that for noninteracting electrons ($U = 0$) and $t = 0$ the electrons would be unable to move as well and the system would be an insulator. However, any arbitrarily small value of t would immediately lead to the formation of a band and a Fermi surface, whereas in the presence of a large U switching on $t \ll U$ would not change the insulating nature of the ground state.

The discussion above already shows one of the reasons why the problem of the Mott-insulator is so difficult. Whereas the ground state for $U = 0$ is unique and easy to write down – the filled Fermi sea – a well-defined ground state for $U/t = \infty$ does not even exist: namely in this limit each site is occupied by one electron, which can have a spin of $\sigma = \pm\frac{1}{2}$. The way in which the spins are distributed over the sites is not determined, however, and for $N_\uparrow = N_\downarrow = N/2$ the number of ways to distribute the $\uparrow$-spins (which automatically fixes the $\downarrow$-spins) is

$$n_d = \binom{N}{N_\uparrow} \approx \sqrt{\frac{2}{\pi N}}\, 2^N,$$

where the Stirling formula has been used. This shows the enormous degree of degeneracy.

If we reduce U/t from infinity to a large but finite value, the spins on the individual sites start to 'communicate' with each other via the process shown in Figure 1. An electron from site i may hop to a neighbor j and form an intermediate state with an empty orbital at i and a doubly occupied orbital at j, see Fig. 1(b). Since the energy of this intermediate state is U, it will be short lived and one of the two electrons in j will hop to the empty site i, resulting in one of the two states in Fig. 1(c). The upper state is identical to the initial state, Fig. 1(a), but there is a gain in kinetic energy of order t^2/U due to the back-and-forth hopping of the electron. Since this back-and-forth hopping is possible only if the spins at i and j are antiparallel to each other, it is energetically favorable if spins on nearest neighbors are antiparallel. In the lower of

the two states in Fig. 1(c) both spins have flipped their direction as compared to Fig. 1(a), so that the spins in the Mott insulator are not static, but have a dynamics of their own. A more quantitative treatment shows that the 'virtual' hopping processes in Fig. 1 can be described by the *Heisenberg antiferromagnet*

$$H_{HAF} = J \sum_{\langle i,j \rangle} \mathbf{S}_i \cdot \mathbf{S}_j = J \sum_{\langle i,j \rangle} \left(S_i^z S_j^z + \frac{1}{2} \left(S_i^+ S_j^- + S_i^- S_j^+ \right) \right). \tag{2}$$

Here $J = 4t^2/U$, $\sum_{\langle i,j \rangle}$ denotes a sum over all $2N$ nearest neighbor pairs, and $\mathbf{S}_i$ is the operator of electron spin at site i, and the spin raising and lowering operators $S^{\pm} = S_x \pm iS_y$ have been introduced to rewrite the term $S_{i,x}S_{j,x} + S_{i,y}S_{j,y}$. Although the electrons in a Mott insulator are localized, their spins therefore acquire a 'life of their own', that means a nontrivial ground state and a spectrum of *spin-excitations*. This problem is even compounded by doping the system, that means removing electrons and thus create mobile vacancies. The appropriate model to describe this is the famous t-J *model*

$$H_{t-J} = -t \sum_{\langle i,j \rangle} \sum_{\sigma} \left(\hat{c}_{i,\sigma}^{\dagger} \hat{c}_{j,\sigma} + H.c. \right) + J \sum_{\langle i,j \rangle} \mathbf{S}_i \cdot \mathbf{S}_j, \tag{3}$$

where the *Hubbard operator* $\hat{c}_{i,\sigma}^{\dagger} = c_{i,\sigma}^{\dagger}(1 - n_{i,\bar{\sigma}})$ creates an electron only on an empty site. The t-J model was originally derived rigorously as the strong coupling version of the Hubbard model by Chao, Spałek, and Oleś [2], and later shown to be the proper theoretical description of the CuO_2 planes in cuprate superconductors by Zhang and Rice [3]. For application to the CuO_2 planes, the appropriate parameter values are $t \approx 350\,\text{meV}$ and $J \approx 140\,\text{meV}$, so $J/t = 0.4$. The Hilbert space of the t-J model consists of states where each site is occupied either by a vacancy or a spin. The first term exchanges a vacancy and a spin on nearest neighbors, the second term is the Heisenberg exchange between spins. We therefore expect that the system continues to have spin excitations, but by their very motion through the 'spin background' the vacancies interact with these, which will modify both, the motion of the holes and the dynamics of the spins.

2 Planar model at half-filling

2.1 Magnons

To illustrate these somewhat vague remarks we now discuss the reasonably well understood case of the undoped Heisenberg antiferromagnet, $N_e = N$, and the motion of a single vacancy in a Heisenberg antiferromagnet, $N_e = N-1$. We consider the Hamiltonian Eq. (2) for one electron per site. If only the terms $\propto S_i^z S_j^z$ were present, the ground state of (2) would be the *Néel state*, shown in Figure 2(a). In this state, the square lattice is divided into two *sublattices* whereby all sites of the A-sublattice are occupied by an $\uparrow$-electron, those of the B-sublattice by a $\downarrow$-electron (we assume that the A-sublattice is the one containing the site $(0,0)$). The energy of this state is $2N\left(-\frac{J}{4}\right) = -NJ/2$. The Néel state, however, is not an eigenstate of the full Hamiltonian (2): acting, e.g., with one of the products $\frac{J}{2} S_i^- S_j^+$ contained in the second term

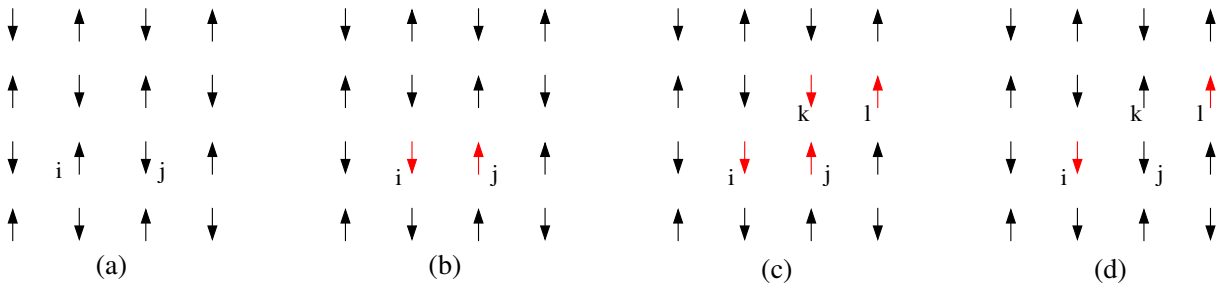

Fig. 2: *The Néel state (a) is* not *the ground state of the Heisenberg antiferromagnet. By acting, e.g., with the term* $\frac{J}{2}\, S_i^- S_j^+$ *in (2) the state (b) is generated, which is orthogonal to the Néel state. Acting further with* $\frac{J}{2}\, S_k^- S_l^+$ *produces (c) and then acting with* $\frac{J}{2}\, S_j^- S_k^+$ *gives (d).*

in (2), the spins at the sites i and j are inverted, resulting in the state shown in Figure 2(b) which is orthogonal to the Néel state. Interestingly, the inverted spins have very much the character of particles in that they can propagate: first, the term $\frac{J}{2}\, S_k^- S_l^+$ appends two additional inverted spins – see Figure 2(c) – and then the term $\frac{J}{2}\, S_j^- S_k^+$ removes two inverted spins, to produce the state in Figure 2(d). The net result of this two-step process is that one of the inverted spins seems to have moved from site j to site l. The particle-like nature of the inverted spins has led to the name *magnons* for them. One can then envisage how this will go on: magnons are created in pairs at various places in the system, then separate and propagate independently by the append-and-remove process, but when two magnons meet they can also 'pair-annihilate' each other by the inverse process Figure 2(b)→(a). There are then two possible outcomes of this scenario: the density of magnons may reach an equilibrium value, where pair-creation and pair annihilations balance each other, so that the underlying antiferromagnetic order persists and we have a Néel state hosting a 'gas of magnons' – or the process may go on until the ordered state is wiped out and we get an entirely new state without order. It turns out that in dimensions $D \geq 2$ the first scenario is realized, and the resulting gas of magnons in antiferromagnetic Mott insulators can be described very well by *linear spin wave theory*. This is frequently derived by means of the Holstein-Primakoff transformation [4] but for the extreme quantum limit of spin $1/2$, which we are considering here, a simpler and more transparent derivation is possible.

We interpret the Néel state in Figure 2(a) as the vacuum state $|0\rangle$ for magnons and model an inverted spin at the site i of the A sublattice by the presence of a Boson, created by $a_i^\dagger$. Similarly, an inverted spin on the site j of the B sublattice is modeled by the presence of a Boson created by $b_j^\dagger$. The state in Figure 2(b) thus would be represented as $a_i^\dagger b_j^\dagger |0\rangle$. We use Bosons to represent the magnons because spin-flip operators such as S_i^+ and S_j^- commute for different sites i and j and these are the operators which create or annihilate the magnons. Since any given spin can be inverted only once, a state like $(a_i^\dagger)^2|0\rangle$ is meaningless. Accordingly, we have to impose the constraint that at most one Boson can occupy a given site. This is equivalent to an infinitely strong on-site repulsion between the magnons and we call this the *hard-core constraint*. An inverted spin on either sublattice is parallel to its $z = 4$ nearest neighbors and the energy changes from $-J/4$ to $+J/4$ for each of these z bonds. Accordingly, we ascribe an energy of formation of $zJ/2$ to each Boson. The spin-flip part creates or annihilates pairs of magnons on

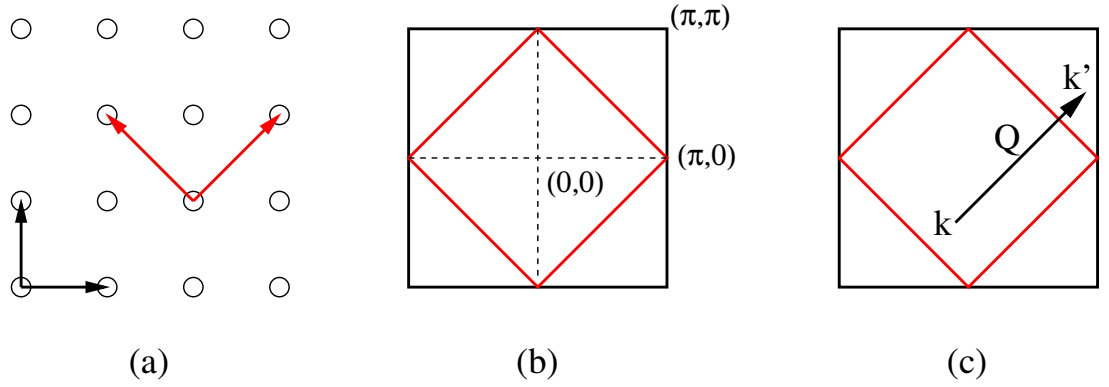

Fig. 3: *(a) The ordered moments in the Néel state make the two sublattices inequivalent, so that the new lattice vectors connect only the sites of one sublattice. The new unit cell is rotated by 45^o and has twice the size of the original one. (b) Accordingly, the new Brillouin zone is rotated by 45^o as well and has half the size of the original one. (c) Every vector* $\mathbf{k}'$ *outside the antiferromagnetic Brillouin zone can be written as* $\mathbf{k}' = \mathbf{k} + \mathbf{Q}$ *with a* $\mathbf{k}$ *inside the zone.*

nearest neighbors, with the matrix element being $J/2$, so that the Hamiltonian for the magnons becomes

$$H_{SW} = \frac{zJ}{2}\left(\sum_{i\in A} a_i^\dagger\, a_i + \sum_{i\in B} b_i^\dagger\, b_i\right) + \frac{J}{2}\sum_{i\in A}\sum_{\mathbf{n}}\left(a_i^\dagger\, b_{i+\mathbf{n}}^\dagger + b_{i+\mathbf{n}}\, a_i\right). \tag{4}$$

Here $\mathbf{n}$ are the z vectors which connect a given site with its z nearest neighbors. In fact, we have made a slight mistake in writing down (4): when two inverted spins reside on nearest neighbors, the number of frustrated bonds is $2z-1$ rather than $2z$. This could be incorporated into H_{SW} as an attractive interaction between magnons on nearest neighbors, but here we ignore this.
The Hamiltonian (4) is a quadratic form but we recall that the Bosons are not free particles, but have to obey the hard-core constraint. However, for the moment we ignore this and treat the Bosons as if they were free particles – we will return to this issue later on. Fourier transforming (4) then gives

$$H_{SW} = \frac{zJ}{2}\sum_{\mathbf{k}}\left(a_{\mathbf{k}}^\dagger a_{\mathbf{k}} + b_{\mathbf{k}}^\dagger b_{\mathbf{k}} + \gamma_{\mathbf{k}}\left(a_{\mathbf{k}}^\dagger b_{-\mathbf{k}}^\dagger + b_{-\mathbf{k}} a_{\mathbf{k}}\right)\right) \tag{5}$$

with

$$a_{\mathbf{k}}^\dagger = \sqrt{\frac{2}{N}}\sum_{j\in A} e^{i\boldsymbol{k}\cdot\boldsymbol{R}_j} a_j^\dagger \quad \text{and} \qquad \gamma_{\mathbf{k}} = \frac{1}{z}\sum_{\mathbf{n}} e^{i\mathbf{k}\cdot\mathbf{n}} = \frac{1}{4}\big(2\cos(k_x) + 2\cos(k_y)\big).$$

Here $\mathbf{k}$ is a wave vector in the antiferromagnetic Brillouin zone (AFBZ), see Figure 3. We can solve (5) by a *Bosonic Bogoliubov transformation*, i.e., we make the ansatz

$$\begin{array}{rcl} \alpha_{\mathbf{k}}^\dagger &=& u_{\mathbf{k}}\;\; a_{\mathbf{k}}^\dagger + v_{\mathbf{k}}\, b_{-\mathbf{k}}, \\ \beta_{-\mathbf{k}}^\dagger &=& u_{\mathbf{k}}\, b_{-\mathbf{k}}^\dagger + v_{\mathbf{k}}\;\; a_{\mathbf{k}}, \end{array} \quad \Rightarrow \quad \begin{array}{rcl} a_{\mathbf{k}}^\dagger &=& u_{\mathbf{k}}\, \alpha_{\mathbf{k}}^\dagger - v_{\mathbf{k}}\, \beta_{-\mathbf{k}}, \\ b_{-\mathbf{k}} &=& -v_{\mathbf{k}}\;\; \alpha_{\mathbf{k}}^\dagger + u_{\mathbf{k}}\, \beta_{-\mathbf{k}}. \end{array} \tag{6}$$

Demanding that $[\alpha_{\mathbf{k}}, \alpha_{\mathbf{k}}^\dagger] = [\beta_{\mathbf{k}}, \beta_{\mathbf{k}}^\dagger] = 1$ gives the condition $u_{\mathbf{k}}^2 - v_{\mathbf{k}}^2 = 1$, which actually has been used to revert the equations on the left hand side of (6) to obtain the right-hand side. Next,

we demand that when expressed in terms of the $\alpha_{\mathbf{k}}^\dagger$ and $\beta_{\mathbf{k}}^\dagger$ the Hamiltonian takes the form

$$H = \sum_{\mathbf{k}} \omega_{\mathbf{k}} \left(\alpha_{\mathbf{k}}^\dagger \alpha_{\mathbf{k}} + \beta_{\mathbf{k}}^\dagger \beta_{\mathbf{k}} \right) + \text{const.}$$

It follows that $[H, \alpha_{\mathbf{k}}^\dagger] = \omega_{\mathbf{k}} \alpha_{\mathbf{k}}^\dagger$. We now insert the *ansatz* (6) into this equation, use the Bosonic commutation relations for $a^\dagger$ and $b^\dagger$, and equate the coefficients of $a_{\mathbf{k}}^\dagger$ and $b_{-\mathbf{k}}$ on both sides of the resulting equation. This leads to the following non-Hermitean eigenvalue problem

$$\begin{pmatrix} \frac{zJ}{2} & -\gamma_{\mathbf{k}} \\ \gamma_{\mathbf{k}}^* & -\frac{zJ}{2} \end{pmatrix} \begin{pmatrix} u_{\mathbf{k}} \\ v_{\mathbf{k}} \end{pmatrix} = \omega_{\mathbf{k}} \begin{pmatrix} u_{\mathbf{k}} \\ v_{\mathbf{k}} \end{pmatrix}. \tag{7}$$

The eigenvalues and eigenvectors of (7) are easily calculated and one finds

$$\omega_{\mathbf{k}} = \frac{zJ}{2} \sqrt{1-\gamma_{\mathbf{k}}^2}, \quad \text{and} \qquad u_{\mathbf{k}} = \sqrt{\frac{1+\nu_{\mathbf{k}}}{2\nu_{\mathbf{k}}}}\,, \quad v_{\mathbf{k}} = \sqrt{\frac{1-\nu_{\mathbf{k}}}{2\nu_{\mathbf{k}}}}, \tag{8}$$

where $\nu_{\mathbf{k}} = \sqrt{1-\gamma_{\mathbf{k}}^2}$. In particular, for $\mathbf{k} \to 0$ we find $\gamma_{\mathbf{k}} \to 1 - (k_x^2+k_y^2)/4 = 1-\mathbf{k}^2/4$ so that $\nu_{\mathbf{k}} \to |\mathbf{k}|/\sqrt{2}$ and $\omega_{\mathbf{k}} \to J\sqrt{2}|\mathbf{k}|$. This shows that the spin waves reach zero frequency at $\mathbf{k} = (0,0)$ and have a cone-shaped dispersion in the neighborhood.

Spin waves can be observed experimentally by inelastic neutron scattering (INS) which, as scattering experiments usually do [5], ultimately measures a dynamical correlation function, in the case of INS the *dynamical spin correlation function* $S(\mathbf{k},\omega)$. Denoting the eigenstates of the system under consideration by $|\nu\rangle$ (with ν=0 the ground state) then at zero temperature it is given by

$$S(\mathbf{k},\omega) = \sum_{\nu} \left| \langle \nu | S_{\mathbf{k}}^+ | 0 \rangle \right|^2 \delta\big(\omega - (E_\nu - E_0)\big), \quad \text{with} \qquad S_{\mathbf{k}}^+ = \frac{1}{\sqrt{N}} \sum_i e^{i\mathbf{k}\cdot\mathbf{R}_i}\, S_i^+.$$

This expression describes the following scattering process: initially, the sample is in its ground state $|0\rangle$ with energy E_0 and $S_z = 0$. A neutron enters the sample with wave vector $\mathbf{K}$, kinetic energy T, and spin $\uparrow$. Its magnetic moment interacts with that of the spin density of a $\downarrow$-electron in some atomic wave function $|\phi_i\rangle$, so that both, the electron and the neutron, flip their spins. The sample remains in an excited state $|\nu\rangle$ with momentum $\mathbf{k}$, energy E_ν and $S_z = 1$, whereas the neutron leaves the sample with wave vector $\mathbf{K} - \mathbf{k}$, energy $T - (E_\nu - E_0)$ and spin $\downarrow$. In our case, the $|\nu\rangle$ are the eigenstates of the spin wave Hamiltonian, so we need to translate the spin operator $S_{\mathbf{k}}^+$ into 'spin wave language'. The operator S_i^+ raises the spin at site i, so if i belongs to the B-sublattice S_i^+ creates a magnon, $S_i^+ = b_i^\dagger$, whereas if i belongs to the A-sublattice S_i^+ annihilates a magnon, $S_i^+ = a_i$. Accordingly we have

$$S_{\mathbf{k}}^+ = \frac{1}{\sqrt{N}} \sum_{i\in A} e^{i\mathbf{k}\cdot\mathbf{R}_i}\, a_i + \frac{1}{\sqrt{N}} \sum_{i\in B} e^{i\mathbf{k}\cdot\mathbf{R}_i}\, b_i^\dagger = \frac{1}{\sqrt{2}} \big(a_{-\mathbf{k}} + b_{\mathbf{k}}^\dagger\big) = \frac{1}{\sqrt{2}} \big(u_{\mathbf{k}} - v_{\mathbf{k}}\big) \big(\alpha_{-\mathbf{k}} + \beta_{\mathbf{k}}^\dagger\big),$$

where the inverse transformation in (6) was used in the last step as well as $u_{-\mathbf{k}} = u_{\mathbf{k}}$ and $v_{-\mathbf{k}} = v_{\mathbf{k}}$. When acting onto the magnon vacuum $|0\rangle$, the term $\propto \alpha_{-\mathbf{k}}$ gives nothing, whereas the term $\propto \beta_{\mathbf{k}}^\dagger$ creates a single magnon. The possible final states $|\nu\rangle$ thus are $\beta_{\mathbf{k}}^\dagger |0\rangle$ with energy

$E_\nu = E_0 + \omega_{\mathbf{k}}$. However, using this expression for all momenta in the Brillouin zone, we would be making a mistake: namely the momenta $\mathbf{k}$ of the magnons in (6) are restricted to the AFBZ whereas the momentum transfer $\mathbf{k}$ in the scattering experiment can be anywhere in the whole Brillouin zone. This is easily remedied, however, if we note that each momentum $\mathbf{k}'$ outside the AFBZ can be written as $\mathbf{k} + \mathbf{Q}$, with $\mathbf{Q} = (\pi, \pi)$ and $\mathbf{k}$ within the AFBZ, see Figure 3(c). Since $e^{i\mathbf{Q}\cdot\mathbf{R}_i} = 1$ for all sites of the A-sublattice (remember that the A-sublattice was the one containing $(0,0)$) and $e^{i\mathbf{Q}\cdot\mathbf{R}_i} = -1$ for all states of the B-sublattice, we have $S^+_{\mathbf{k}+\mathbf{Q}} = (a_{-\mathbf{k}} - b^\dagger_{\mathbf{k}})/\sqrt{2} = (u_{\mathbf{k}} + v_{\mathbf{k}})(\alpha_{-\mathbf{k}} - \beta^\dagger_{\mathbf{k}})/\sqrt{2}$. Inserting everything we find

$$S(\mathbf{k},\omega) = \frac{1}{2}\big(u_{\mathbf{k}} - v_{\mathbf{k}}\big)^2\, \delta(\omega - \omega_\nu), \qquad S(\mathbf{k}+\mathbf{Q},\omega) = \frac{1}{2}\big(u_{\mathbf{k}} + v_{\mathbf{k}}\big)^2\, \delta(\omega - \omega_\nu).$$

Let us assume that the momentum transfer is $\boldsymbol{k} = \mathbf{Q} + \delta\mathbf{k}$ or $\boldsymbol{k} = \delta\mathbf{k}$, with a small $\delta\mathbf{k}$. In both cases, $\omega_{\boldsymbol{k}} \to J\sqrt{2}|\delta\mathbf{k}|$, whereas the square of the scattering matrix element

$$\big|\langle\nu|S^+_{\mathbf{k}}|0\rangle\big|^2 = \frac{1}{2}\big(u_{\delta\mathbf{k}} \pm v_{\delta\mathbf{k}}\big)^2 = \frac{1}{2}\,\frac{1 \pm |\gamma_{\delta\mathbf{k}}|}{\sqrt{1-\gamma^2_{\delta\mathbf{k}}}} \to \begin{cases} \dfrac{\sqrt{2}}{|\delta\mathbf{k}|} & , + \\[2ex] \dfrac{|\delta\mathbf{k}|}{4\sqrt{2}} & , - \end{cases}$$

The matrix element, which gives the peak-intensity in the inelastic neutron spectrum, thus approaches zero for momentum transfer 0, but diverges for momentum transfer $\mathbf{Q}$. A comparison to an actual INS experiment is shown in Figure 4. It is quite obvious that the agreement with experiment is excellent, both with respect to the spin wave dispersion and the $\mathbf{k}$-dependence of the peak intensity, and in fact spin wave theory is a highly successful description of the properties of antiferromagnetic Mott insulators. The bandwidth of $\omega_{\mathbf{k}}$ is roughly $300\,\text{meV}$ and from (8) one can see that spin wave theory predicts a bandwidth of $2J$, so $J \approx 150\,\text{meV}$. This is slightly larger than the value given above, but to get a really good fit the authors of Ref. [6] actually have included an additional ring exchange term whereas their nearest neighbor $J = 138m\,\text{meV}$.
To conclude this section, we return to the issue of the hard-core constraint which the $a^\dagger$ and $b^\dagger$ Bosons had to obey and which we had simply ignored. To address this question, we calculate the density of these Bosons, i. e.,

$$n_a \;=\; \frac{2}{N}\sum_{\mathbf{k}} \big\langle a^\dagger_{\mathbf{k}} a_{\mathbf{k}}\big\rangle = \frac{2}{N}\sum_{\mathbf{k}} v^2_{\mathbf{k}} = \frac{2}{N}\sum_{\mathbf{k}} \frac{1-\nu_{\mathbf{k}}}{2\nu_{\mathbf{k}}}.$$

Numerical evaluation for a 2D square lattice gives $n_a = 0.19$. The probability that two of the Bosons occupy the same site and violate the constraint therefore is $\approx n_a^2 = 0.04 \ll 1$ and our assumption of relaxing the constraint is justified a posteriori.
Summarizing the discussion so far we have seen that in a Mott-insulator the sites carry a spin of $\pm\frac{1}{2}$. These spins can communicate with each other by means of virtual charge fluctuations and this is described by the Heisenberg antiferromagnet. In dimensions $D \geq 2$ this leads to antiferromagnetic order in the ground state and a new type of excitations, magnons or spin waves, which correspond to spins standing opposite to the antiferromagnetic order.

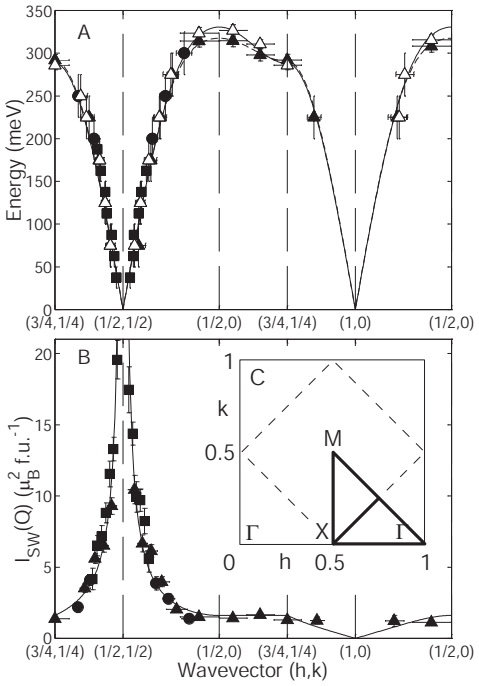

Fig. 4: *Comparison of spin wave theory to INS results for La_2CuO_4. The top part shows the dispersion of the frequency $\omega_{\mathbf{k}}$ of the spin waves, the bottom part the* **k***-dependence of the peak intensity $\propto (u_{\mathbf{k}} \pm v_{\mathbf{k}})^2$. In this Figure, wave vectors* **k** *are given in units of $2\pi/a$, so that the authors' $(1,0)$ is our $(0,0)$ (but measured in the 2nd zone to avoid looking into the incoming beam) whereas $(\frac{1}{2},\frac{1}{2})$ is our (π,π). The dots are experimental data, the lines the prediction of spin wave theory. Note the cone-shaped dispersion around $(0,0)$ and (π,π) and the divergence/vanishing of the spectral weight at these points. Reprinted with permission from [6], Copyright 2001 by the American Physical Society.*

2.2 One hole in an antiferromagnet

Let us next consider the first step of 'doping the system' and consider the case of a single vacancy in a system described by the t-J model, Eq. (3). A single hole will not change the magnetic order due to interaction of the remaining $N-1$ spins, so we assume antiferromagnetic order and decompose the t-J Hamiltonian Eq. (3) as $H = H_t + H_I + H_\perp$ whereby

$$H_t = -t \sum_{\langle i,j \rangle} \sum_{\sigma} \left(\hat{c}^\dagger_{i,\sigma} \hat{c}_{j,\sigma} + H.c \right), \quad H_I = J \sum_{\langle i,j \rangle} S^z_i S^z_j, \quad H_\perp = \frac{J}{2} \sum_{\langle i,j \rangle} \left(S^+_i S^-_j + H.c. \right),$$

and choose $H_0 = H_t + H_I$ as our unperturbed Hamiltonian. As already stated, in the absence of any hole the ground state of H_0 is the Néel state with energy $E_N = -NJ/2$. If now an electron is removed from site i belonging to the $\uparrow$-sublattice – see Figure 5(a). This raises the exchange energy by $zJ/4$, because z bonds change their energy from $-J/4$ to 0. We choose the exchange energy of the resulting state, $E_N + zJ/4$, as the zero of energy. Then, the hopping term in (3) can become active and the spin from a neighboring site i_1 is transferred to i, resulting in the state in Figure 5(b). Since the shifted spin has 'switched sublattices', however, it now is opposite to the antiferromagnetic order. In fact, this inverted spin at site i is nothing but a magnon as

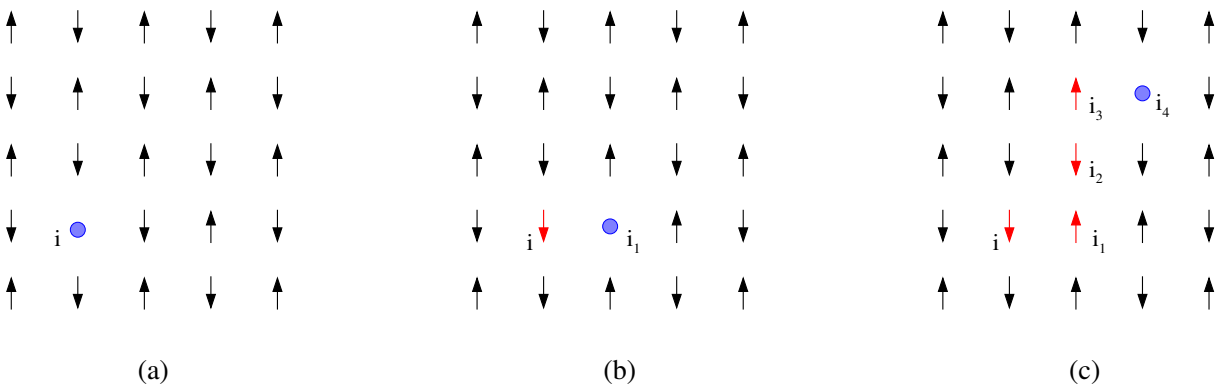

(a) (b) (c)

Fig. 5: *A hole hopping in the Néel state creates a 'string' of misaligned spins.*

discussed in the preceding section, so that the hopping vacancy 'radiates off' magnons [7, 8]. Since the displaced spin at site i is parallel to $z-1$ neighbors, the exchange energy increases by $(z-1)J/2$. And this continues as the vacancy moves through the Néel state, see Figure 5(c): in each step another spin is shifted to the opposite sublattice, so that the vacancy leaves behind a trace of misaligned spins and the exchange energy increases roughly linearly with the distance travelled by the hole. We call a state which is created by the motion of a vacancy in the Néel state a 'string state' and denote it by $|i_0, i_1, \ldots, i_\nu\rangle$. Here i_0 is the site where the hole was created, $i_1, i_2, i_{\nu-1}$ are the sites visited by the hole, whereas i_ν is the site where the vacancy is located. We call ν the length of the string, for example Figure 5(c) shows a string of length 4. There are z different string states with $\nu = 1$, whereas in any subsequent hop starting from a string state of length ν, $z-1$ new string states of length $\nu+1$ are generated. The number of different strings of length ν therefore is $n_\nu = z(z-1)^{\nu-1}$ for $\nu \geq 1$ whereas $n_0 = 1$. Since each displaced spin is parallel to $z-2$ neighbors – see Figure 5 – the magnetic energy increases by $J(z-2)/2$ per displaced spin, except for the first hop away from i where it increases by $J(z-1)/2$. Accordingly, the exchange energy for a string of length $\nu > 0$ his

$$I_\nu = \frac{(z-1)J}{2} + (\nu-1)\,\frac{(z-2)J}{2} = \frac{J}{2}\big((z-1) + (\nu-1)(z-2)\big), \tag{9}$$

and $I_0 = 0$. It may happen that the path which the hole has taken is folded or self-intersecting in which case (9) clearly is not correct. However it will be correct for 'most' possible paths of the hole, in particular it is correct for $\nu \leq 2$ so that we will use this expression. Neglecting the possibility of self-intersection or folding of the string is an approximation known as *Bethe-lattice*. Since the magnetic energy increases linearly with the number of hops the hole has taken, we conclude that under the action of H_0 the hole is self-trapped. To describe the resulting localized state we make the following *ansatz*

$$|\Phi_i\rangle = \sum_{\nu=0}^{\infty} \alpha_\nu \sum_{i_1, i_2, \ldots, i_\nu} |i, i_1, i_2, \ldots, i_\nu\rangle, \tag{10}$$

where it is understood that the second sum runs only over those ν-tuples of sites which correspond to a true string starting at i. Since we assume that the magnetic energy is the same for all

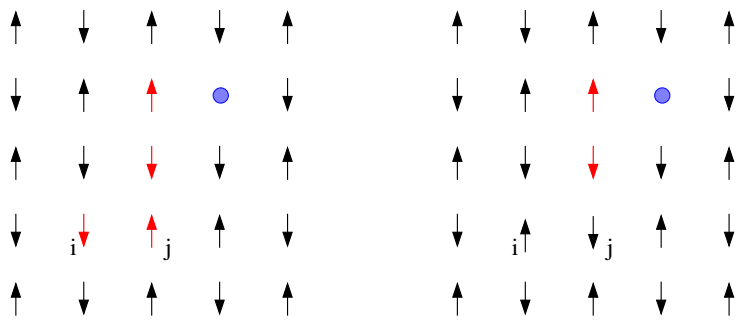

Fig. 6: *By acting with the term $\frac{J}{2}\, S_i^+ S_j^-$ the first two defects created by the hole can be 'healed' and the starting point of the string be shifted to a neighbor.*

strings of length ν, the coefficient α_ν depends only on the length of the string. The coefficients α_ν in (10) are to be determined by minimizing the expectation value of H_0. The norm and magnetic energy are

$$\langle \Phi_i | \Phi_i \rangle = \sum_{\nu=0}^{\infty} n_\nu \alpha_\nu^2 \quad = \sum_{\nu=0}^{\infty} \beta_\nu^2, \tag{11}$$

$$\langle \Phi_i | H_I | \Phi_i \rangle = \sum_{\nu=0}^{\infty} n_\nu I_\nu \alpha_\nu^2 \; = \sum_{\nu=0}^{\infty} I_\nu \beta_\nu^2, \tag{12}$$

where we have introduced $\beta_\nu = \alpha_\nu / \sqrt{n_\nu}$. To obtain the expectation value of the kinetic energy we consider a string state of length $\nu \geq 1$ which has the coefficient α_ν. By acting with the hopping term we obtain $z-1$ strings of length $\nu+1$, with coefficient $\alpha_{\nu+1}$, and 1 string of length $\nu-1$, with coefficient $\alpha_{\nu-1}$. For $\nu = 0$ we obtain z strings of length 1. In this way we find

$$\langle \Phi_i | H_t | \Phi_i \rangle = t \Big(z\alpha_0\alpha_1 + \sum_{\nu=1}^{\infty} n_\nu \alpha_\nu \big(\alpha_{\nu-1} + (z-1)\alpha_{\nu+1} \big) \Big) = 2t \sum_{\nu=0}^{\infty} n_{\nu+1} \alpha_\nu \alpha_{\nu+1} = 2 \sum_{\nu=0}^{\infty} \tilde{t}_\nu \, \beta_\nu \beta_{\nu+1}, \tag{13}$$

where $\tilde{t}_0 = \sqrt{z}\, t$ and $\tilde{t}_\nu = \sqrt{z-1}\, t$ for $\nu > 0$. The prefactor on the right-hand side is t instead of $-t$ as one might have expected from (3) because the hopping term has to be rearranged as $-t\, \hat{c}^\dagger_{i,\sigma} \hat{c}_{j,\sigma} = t\, \hat{c}_{j,\sigma} \hat{c}^\dagger_{i,\sigma}$ to describe the hopping of a hole. As already stated, the β_ν now are determined from the requirement that the expectation value $E_{loc} = \langle \Phi_i | H_0 | \Phi_i \rangle / \langle \Phi_i | \Phi_i \rangle$ be stationary under variation of each β_ν

$$\begin{aligned} \frac{\partial E_{loc}}{\partial \beta_\nu} &= \frac{1}{\langle \Phi_i | \Phi_i \rangle^2} \left[\frac{\partial \langle \Phi_i | H_0 | \Phi_i \rangle}{\partial \beta_\nu} \langle \Phi_i | \Phi_i \rangle - \langle \Phi_i | H_0 | \Phi_i \rangle \frac{\partial \langle \Phi_i | \Phi_i \rangle}{\partial \beta_\nu} \right] \\ &= \frac{1}{\langle \Phi_i | \Phi_i \rangle} \left[\frac{\partial \langle \Phi_i | H_0 | \Phi_i \rangle}{\partial \beta_\nu} - E_{loc} \frac{\partial \langle \Phi_i | \Phi_i \rangle}{\partial \beta_\nu} \right] = 0. \end{aligned}$$

Setting the square bracket equal to zero and using Eqs. (11), (12), and (13) we obtain [9]

$$\big(\tilde{t}_\nu \beta_{\nu+1} + \tilde{t}_{\nu-1} \beta_{\nu-1} \big) + I_\nu \beta_\nu = E_{loc} \beta_\nu,$$

with the boundary condition $\beta_{-1} = 0$. This results in a tridiagonal Hamilton matrix for the β_ν and after cutting off at a sufficiently large ν, E_{loc} and the βs can be obtained by a simple numerical matrix diagonalization.

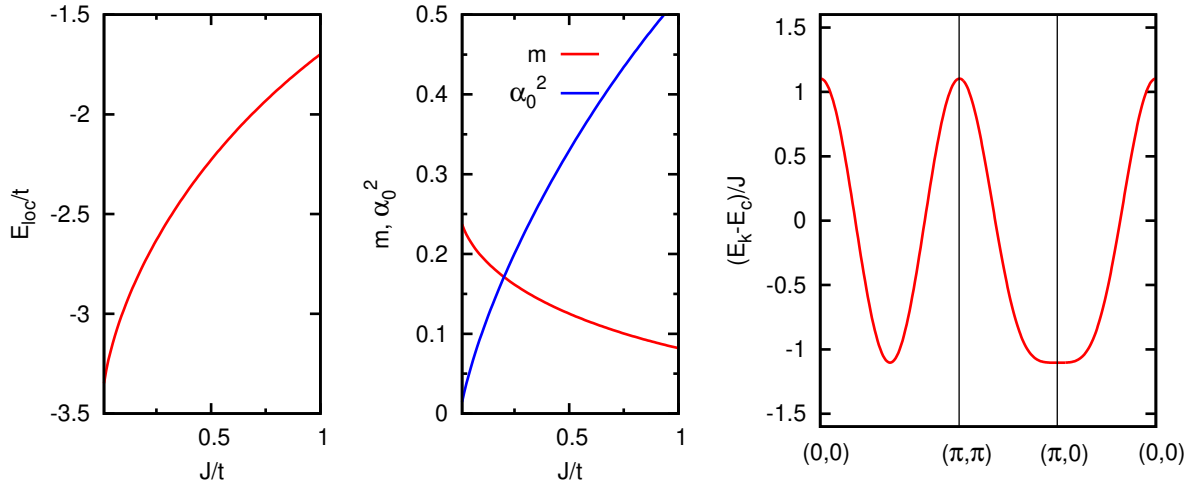

Fig. 7: *Left: Energy of the self-trapped state E_{loc} versus J/t. Center: Matrix element m due to string truncation and renormalization factor α_0^2 for the t' and t'' hopping terms versus J/t. Right: Band structure $E_{\boldsymbol{k}}$ for $J/t = 0.4$.*

So far it seems that the hole in the Néel state is localized. It is easy to see, however, that the term $H_\perp$ which we have neglected so far can assist the trapped hole in escaping from the string potential, see Figure 6. Namely by acting on the first two sites of a string, the spins which were inverted by the hole are inverted a second time and thus fit with the Néel order again: $H_\perp|i, i_1, i_2, i_3, \ldots, i_\nu\rangle = \frac{J}{2}\ |i_2, i_3, \ldots, i_\nu\rangle$. The initial site of the string thus is shifted to a $(2,0)$- or $(1,1)$-like neighbor while simultaneously the length ν is decreased by two. The term $H_\perp$ may also append two new defects to a string, $H_\perp|i_2, i_3, \ldots, i_\nu\rangle = \frac{J}{2}\ |i, i_1, i_2, i_3, \ldots, i_\nu\rangle$ thus increasing the length by 2 and again shifting the starting point to a $(2,0)$- or $(1,1)$-like neighbor. Using again the Bethe lattice approximation we find the matrix element

$$\langle\Phi_{i+2\hat{x}}|H_\perp|\Phi_i\rangle = J\sum_{\nu=0}^{\infty}(z-1)^\nu\ \alpha_\nu\alpha_{\nu+2} = \frac{J}{z}\left(\sqrt{\frac{z}{z-1}}\,\beta_0\beta_2 + \sum_{\nu=1}^{\infty}\beta_\nu\beta_{\nu+2}\right) = J\cdot m,$$

whereas $\langle\Phi_{i+\hat{x}+\hat{y}}|H_\perp|\Phi_i\rangle = 2J\cdot m$ because a string to a $(1,1)$-like neighbor can pass either trough $(1,0)$ or $(0,1)$ and the contributions from these two different paths are additive.
When the full Hamiltonian $H_0 + H_\perp$ is taken into account the hole therefore can propagate through the entire lattice and we describe this by the Bloch state

$$|\Phi_{\mathbf{k}}\rangle \ = \ \sqrt{\frac{2}{N}}\sum_{j\in A} e^{-i\mathbf{k}\cdot\mathbf{R}_j}\ |\Phi_i\rangle. \tag{14}$$

This is reminiscent of an LCAO wave function such as (1), but the role of the atomic orbital $|\phi_i\rangle$ here is played by the self-trapped function $|\Phi_i\rangle$. Since the matrix element of $H_\perp$ between $(1,1)$-like neighbors is twice that between $(2,0)$-like neighbors we obtain the dispersion

$$\begin{aligned} E_{\mathbf{k}} &= E_{loc} + 2Jm\cdot 4\cos(k_x)\cos(k_y) + Jm\cdot 2\big(\cos(2k_x)+\cos(2k_y)\big) \\ &= E_{loc} - 4Jm + 4Jm\big(\cos(k_x)+\cos(k_y)\big)^2 \end{aligned} \tag{15}$$

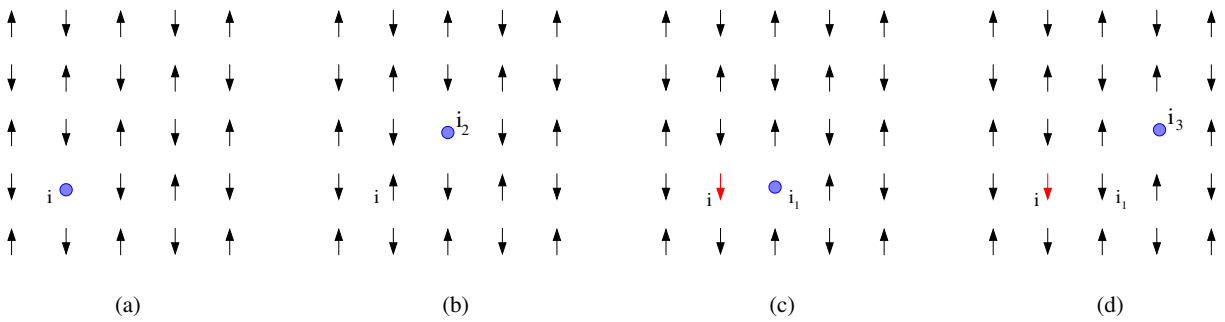

Fig. 8: *Hopping processes involving a term* $\propto t'$ *that connects* $(1,1)$*-like neighbors.*

This expression shows several remarkable features which reflect the unusual nature of hole motion. First, there is the constant term $E_{loc} \propto t$. As we have seen, in the absence of the spin-flip term $H_\perp$, the hole is self-trapped in a linearly ascending 'effective potential' due to magnetic frustration. The hole executes a rapid zig-zag motion on a timescale $\tau_{loc} \propto t^{-1}$, and E_{loc} is the gain of kinetic energy due to this zig-zag motion. Figure 7 shows that $E_{loc} \approx -2.4\,t$ at $J/t = 0.4$, which is an appreciable fraction of $-4t$, the lowest possible kinetic energy which a freely propagating electron can have in an empty $2D$ lattice. On the longer time scale $\tau_{deloc} \propto J^{-1}$, the spin-flip term shifts the center of the zig-zag motion to a 2^{nd} or 3^{rd} nearest neighbor, and the zig-zag motion starts anew. It follows that the bandwidth for coherent motion is *not* proportional to the hopping integral t, but to the smaller exchange constant J. The total bandwidth is $16Jm$ and since m is around 0.14 for $J/t = 0.4$ – see Figure 7 – the bandwidth is roughly $2J$. With $J = 140$ meV as appropriate for cuprates, we expect $W \approx 300$ meV, almost a factor of 10 smaller than the width of the free tight-binding dispersion, which is $8t \approx 2.8$ eV. $E_{\mathbf{k}}$ has a degenerate minimum along $(\pi,0) \to (0,\pi)$ and symmetry equivalent lines, its maxima are at $(0,0)$ and (π,π). It has 'antiferromagnetic symmetry', $E_{\mathbf{k}+\mathbf{Q}} = E_{\mathbf{k}}$, which is to be expected since we are considering hole motion in an antiferromagnetic background.

In order to compare our theory to experiment we need to take into account that in the actual CuO_2-planes there are appreciable additional hopping integrals t' between $(1,1)$-like and t'' between $(2,0)$-like neighbors. Since these terms connect pairs of neighbors which are on the same sublattice, they do not create frustration and it might seem that they immediately dominate the hole motion. However, this is not the case and the reason can be seen in the next Figure. Fig. 8(a) shows a 'string of length 0', that means a hole at site i and the hopping term $\propto t'$ can transport the hole to the $(1,1)$-like neighbor i_2 without creating a magnon. On the other hand, 8(c) shows a 'string of length 1', that means a hole which has executed one nearest neighbor hopping process and is now at site i_1, with a single magnon at site i. Again, the t'-term can transport the hole to the $(1,1)$-like neighbor i_3, but it cannot transport the magnon along with the hole. Therefore, the hopping terms $\propto t', t''$ can transport only the 'bare hole', and since this has the coefficient α_0 in the self-trapped states $|\Phi_i\rangle$, these terms are renormalized by a factor α_0^2. Accordingly, they give the following contribution to the hole dispersion relation

$$E_{lr}(\mathbf{k}) = 4t'\alpha_0^2 \cos(k_x)\cos(k_y) + 2t''\alpha_0^2\big(\cos(2k_x) + \cos(2k_y)\big)$$

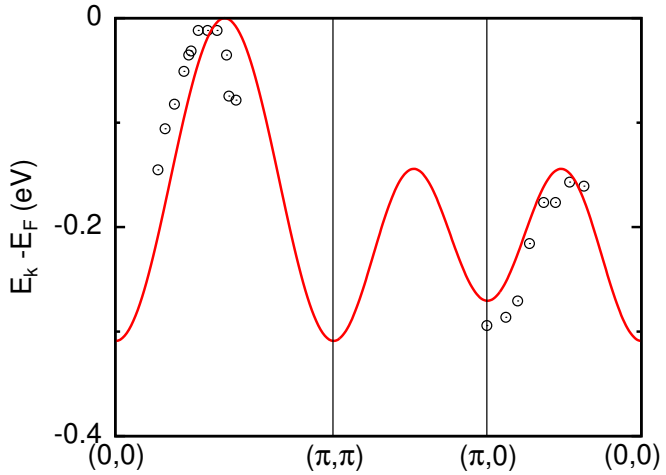

Fig. 9: *The band structure for the t-J model with additional hopping terms compared to the experimental valence band structure for the antiferromagnetic insulator $Sr_2CuO_2Cl_2$ [10]. Parameter values are $t = 350\,meV$, $J = 140\,meV$, $t' = -120\,meV$, and $t'' = 60\,meV$.*

which has to be added to (15). Note again the opposite sign of the hopping terms as compared to the original Hamiltonian (3) because the Fermion operators have to be exchanged to transport a hole. Figure 9 shows a comparison of the modified hole dispersion and the experimental band structure obtained by Angle Resolved Photoemission Spectroscopy (ARPES) on the insulating CuO-compound $Sr_2CuO_2Cl_2$ [10]. The band structure for a hole has to be turned upside down to compare to ARPES because the minimum of the hole-bandstructure is the maximum of the electron-band structure. The agreement is reasonable whereby it has to be kept in mind that in a wide area around (π, π) and also close to $(0, 0)$ the band structure cannot be observed because the band has vanishing spectral weight in ARPES. In any way, the drastic reduction of the bandwidth can be seen clearly.

Looking back, the above discussion illustrates the general remarks in the introduction. In a Mott insulator each site carries a spin and spins on neighboring sites are coupled by the exchange term. This leads to a tendency for neighboring spins to be antiparallel and the appearance of spin excitations, which in the antiferromagnetic phase take the form of spin waves. Doped holes then have to move through this 'spin background' and by their very motion constantly interact with the magnetic excitations. As we have seen this leads to a drastic modification of the hole motion and band structure. And in fact, this also goes the other way round: since the holes are constantly 'stirring' the spins, these react and change their arrangement so as to make hole motion easier and allow for a gain kinetic energy. In cuprate superconductors the antiferromagnetic state which could be described by the above theory breaks down for hole concentrations of only a few per cent. Even in the resulting disordered state, the spin exchange term in the t-J Hamiltonian still favors antiparallel orientation of spins on nearest neighbors and in fact neutron scattering experiments show that there it still has *short range antiferromagnetic order* that means the spin correlation function $\langle \boldsymbol{S}_i \cdot \boldsymbol{S}_{i+\boldsymbol{R}} \rangle \propto e^{i\boldsymbol{Q}\cdot\boldsymbol{R}}\, e^{-|\boldsymbol{R}|/\zeta}$. This is reminiscent of the density correction function in a molten crystal, where locally the correlations between atoms resemble that of the original solid but there is no more long range crystalline order. Accordingly, such a state is called a 'spin liquid' and this is what we want to discuss next.

3 Spin liquids

3.1 Dimer basis

As a prelude we follow Sachdev and Bhatt [11] as well as Gopalan, Rice, and Sigrist [12] and consider a *dimer* of two sites, labeled 1 and 2, and assume that both of them are occupied by one electron each, with their spins coupled by the exchange term $H = J\ \mathbf{S}_1 \cdot \mathbf{S}_2$. According to the rules for addition of angular momenta, the two spins of $\frac{1}{2}$ can be coupled to the total spin $S = 1$ (spin triplet) or $S = 0$ (spin singlet). The singlet and the three components of the triplet are eigenstates of the square of the operator of total spin $\mathbf{S} = \mathbf{S}_1 + \mathbf{S}_2$ with eigenvalue $S(S+1)$: $\mathbf{S}^2 = \mathbf{S}_1^2 + 2\mathbf{S}_1 \cdot \mathbf{S}_2 + \mathbf{S}_2^2 = S(S+1)$, and using that $\mathbf{S}_1^2 = \mathbf{S}_2^2 = \frac{1}{2}\left(\frac{1}{2}+1\right) = \frac{3}{4}$ we find $\mathbf{S}_1 \cdot \mathbf{S}_2 = \frac{1}{2}(S(S+1) - \frac{3}{2})$. Accordingly, $\mathbf{S}_1 \cdot \mathbf{S}_2$ gives $-\frac{3}{4}$ when acting on the singlet and $\frac{1}{4}$ for a triplet. Due to the limited size of the Hilbert space of the dimer, constructing states with definite total spin thus is equivalent to diagonalizing the exchange term, and we find the eigenenergies $-3J/4$ for the singlet, and $J/4$ for the three components of the triplet. The eigenstates themselves can be found by using the standard technique for adding angular momenta and are given by [11, 12]

$$\begin{aligned}
|s\rangle &= \frac{1}{\sqrt{2}} \left(c^\dagger_{1,\uparrow} c^\dagger_{2,\downarrow} - c^\dagger_{1,\downarrow} c^\dagger_{2,\uparrow} \right) |0\rangle, \\
|t_x\rangle &= \frac{1}{\sqrt{2}} \left(c^\dagger_{1,\downarrow} c^\dagger_{2,\downarrow} - c^\dagger_{1,\uparrow} c^\dagger_{2,\uparrow} \right) |0\rangle, \\
|t_y\rangle &= \frac{i}{\sqrt{2}} \left(c^\dagger_{1,\uparrow} c^\dagger_{2,\uparrow} + c^\dagger_{1,\downarrow} c^\dagger_{2,\downarrow} \right) |0\rangle, \\
|t_z\rangle &= \frac{1}{\sqrt{2}} \left(c^\dagger_{1,\uparrow} c^\dagger_{2,\downarrow} + c^\dagger_{1,\downarrow} c^\dagger_{2,\uparrow} \right) |0\rangle. \qquad (16)
\end{aligned}$$

with $|s\rangle$ the singlet and $|t_x\rangle$, $|t_y\rangle$, and $|t_z\rangle$ the three components of the triplet. Thereby the three $|t_\alpha\rangle$ in (16) are *not* eigenstates of the total z-spin – rather they are linear combinations of these eigenstates which obey $S_\alpha |t_\beta\rangle = i\varepsilon_{\alpha\beta\gamma}\ |t_\gamma\rangle$, for example:

$$\begin{aligned}
S_x |t_y\rangle &= \frac{1}{2} \sum_{i=1}^{2} (S_i^- + S_i^+)\ \frac{i}{\sqrt{2}}\ \left(c^\dagger_{1,\uparrow} c^\dagger_{2,\uparrow} + c^\dagger_{1,\downarrow} c^\dagger_{2,\downarrow} \right) \\
&= \frac{i}{2\sqrt{2}} \left(c^\dagger_{1,\downarrow} c^\dagger_{2,\uparrow} + c^\dagger_{1,\uparrow} c^\dagger_{2,\downarrow} + c^\dagger_{1,\uparrow} c^\dagger_{2,\downarrow} + c^\dagger_{1,\downarrow} c^\dagger_{2,\uparrow} \right) = i |t_z\rangle.
\end{aligned}$$

This means that the three states $|t_\alpha\rangle$ transform like a vector under spin rotations which will be convenient later on. We also note that under the exchange of the two sites, $1 \leftrightarrow 2$, we have $|s\rangle \to |s\rangle$ but $|t_\alpha\rangle \to -|t_\alpha\rangle$. Let us now return to the problem of describing a 'spin liquid' and first consider the undoped Heisenberg antiferromagnet on a 2D square lattice with N sites. A state which on one hand is disordered and on the other hand is an exact spin singlet can be obtained in the following way: let the N sites be partitioned into $N/2$ dimers, whereby each dimer comprises two nearest neighbor sites, see Figure 10 (a), and assume moreover that the two spins in each dimer are coupled to form a singlet. This state is a product state

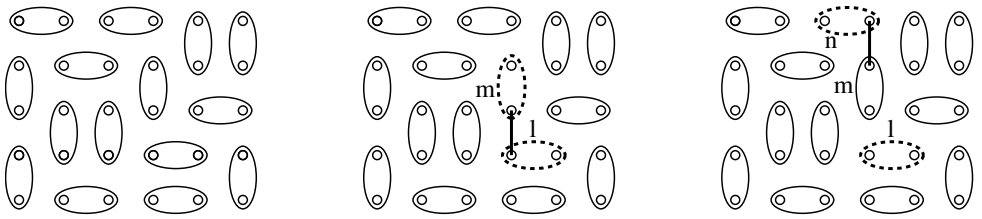

(a) (b) (c)

Fig. 10: *(a) A dimer covering of the plane – spins on sites covered by an ellipse are coupled to a singlet. (b) By acting with the exchange along the bond connecting the dimers l and m both dimers are excited into the triplet state. (c) By acting with the exchange along the bond connecting the dimers m and n bond m is de-excited to the singlet whereas dimer n is excited to the triplet – the triplet has propagated.*

$$|\Psi_0\rangle = \prod_{(i,j)\in D} \frac{1}{\sqrt{2}} \left(c^\dagger_{i,\uparrow} c^\dagger_{j,\downarrow} - c^\dagger_{i,\downarrow} c^\dagger_{j,\uparrow} \right)$$

where D is the set of $N/2$ pairs (i,j) of nearest neighbor sites corresponding to the given dimer covering. $|\Psi_0\rangle$ is an eigenstate of the 'depleted Hamiltonian' $H_d = J \sum_{(i,j)\in D} \mathbf{S}_i \cdot \mathbf{S}_j$ with eigenvalue $E_{d,0} = (N/2)\cdot(-3J/4)$. Since $\langle \mathbf{S}_i \cdot \mathbf{S}_j \rangle = 0$ if i and j belong to different dimers – as will be shown in a moment – this is also the expectation value of the full Hamiltonian in the state $|\Psi_0\rangle$. Next, let us consider what happens if we act onto $|\Psi_0\rangle$ with the exchange along a bond *not included* in the set D, that means a bond connecting spins in different dimers – such as the bond indicated in Figure 10(b). Due to the product nature of $|\Psi_0\rangle$ it is sufficient to discuss what happens when the spin operator acts on a singlet, e.g.,

$$S_{1,x}|s\rangle = \frac{1}{2}\left(S^-_1 + S^+_1\right) \frac{1}{\sqrt{2}} \left(c^\dagger_{1,\uparrow} c^\dagger_{2,\downarrow} - c^\dagger_{1,\downarrow} c^\dagger_{2,\uparrow} \right) |0\rangle = \frac{1}{2\sqrt{2}} \left(c^\dagger_{1,\downarrow} c^\dagger_{2,\downarrow} - c^\dagger_{1,\uparrow} c^\dagger_{2,\uparrow} \right) |0\rangle. \quad (17)$$

Comparing with (16), the expression on the right-hand side is seen to be $\frac{1}{2}|t_x\rangle$. Next, we exchange $1 \leftrightarrow 2$ on both sides of (17), whence $S_{1,x} \to S_{2,x}$, $|s\rangle \to |s\rangle$, and $|t_x\rangle \to -|t_x\rangle$, and obtain $S_{2,x}|s\rangle = -\frac{1}{2}|t_x\rangle$. Since the triplets where constructed to transform like a vector, this holds true for the other Cartesian components as well: $S_{1,\alpha}|s\rangle = \pm\frac{1}{2}|t_\alpha\rangle$, $\alpha \in \{x,y,z\}$. Acting with the term $J\mathbf{S}_i \cdot \mathbf{S}_j$ along a bond which connects sites i and j in different dimers therefore simultaneously excites both dimers to the triplet state, with a prefactor of $\pm J/2$ (the prefactor will be discussed more precisely below). The new state is again an eigenstate of H_d, with eigenvalue $E_{d,0} + 2J$ and obviously is orthogonal to $|\Psi_0\rangle$ – which also proves that the expectation value $\langle \mathbf{S}_i \cdot \mathbf{S}_j \rangle$ vanishes if the sites i and j belong to different dimers. Next, we consider what happens when the exchange term acts along the bond indicated in Figure 10(c). We already know that bond n will be excited to the triplet state but we need to study what happens when the spin operator acts on the triplet in bond m:

$$S_{1,x}|t_x\rangle = \frac{1}{2}\left(S^+_1 + S^-_1\right) \frac{1}{\sqrt{2}} \left(c^\dagger_{1,\downarrow} c^\dagger_{2,\downarrow} - c^\dagger_{1,\uparrow} c^\dagger_{2,\uparrow} \right) |0\rangle = \frac{1}{2\sqrt{2}} \left(c^\dagger_{1,\uparrow} c^\dagger_{2,\downarrow} - c^\dagger_{1,\downarrow} c^\dagger_{2,\uparrow} \right) |0\rangle, \quad (18)$$

which is nothing but $\frac{1}{2}|s\rangle$. Therefore, acting with the exchange term along the bond indicated in Figure 10(c), the dimer m is de-excited to the singlet state according to (18), whereas the

dimer n is excited to the triplet state according to (17). Comparing now with Figure 2 we see a quite analogous pattern arising: both, the Néel state and the dimer state $|\Psi_0\rangle$ are the ground state of a part of the Hamiltonian, namely the longitudinal part $J\sum_{\langle i,j\rangle} S_{i,z}S_{j,z}$ in the case of the Néel state and the depleted Hamiltonian H_d for the dimer state. Switching on the remainder of the Hamiltonian then creates 'fluctuations': these were the inverted spins or magnons in the case of the Néel state, and the excited dimers in the case of the singlet soup. The fluctuations increase the energy: by $zJ/2$ for a magnon, and by J for a triplet. After having been created these fluctuations then propagate through the lattice. This suggests that we proceed as in the case of spin wave theory and interpret the triplets as effective Bosonic particles (we use Bosons because a triplet is composed of two electrons). To be more quantitative, we need to introduce some conventions: We assume that the bonds are labeled by a number $n \in \{1,\ldots,N/2\}$. Since the triplet has negative parity under the exchange of sites, $1 \leftrightarrow 2$, we need to specify which of the sites i and j in a given dimer corresponds to the site 1 in Eq. (16) and which one to the site 2. We adopt the convention that for a bond in x-direction (y-direction) the left (lower) site always corresponds to the site 1. We call the site which corresponds to 1 the 1-site of the dimer and the site which corresponds to 2 the 2-site of the dimer. For each site i we define $\lambda_i = 1$ if it is the 1-site of its respective dimer, and -1 if it is the 2-site. Then, if a given dimer m is occupied by a singlet, we consider it as occupied by a Bosonic particle, created by $s^\dagger_m$, whereas if the dimer is in one of the three triplet states we consider it as occupied by a Boson, created by $t^\dagger_{m,\alpha}$ with $\alpha \in \{x,y,z\}$. We have already seen that the three triplet states transform like a vector under spin rotations and it follows that the corresponding creation operators form a *vector operator* $[S_\alpha, t^\dagger_\beta] = i\varepsilon_{\alpha\beta\gamma}t^\dagger_\gamma$, and by Hermitean conjugation it is found that the annihilation operator $\mathbf{t}_m$ is a vector operator as well. By calculating the action of the spin operator on triplet states we then find the representation of the spin operator

$$\mathbf{S}_j \to \frac{\lambda_j}{2}\left(s^\dagger\mathbf{t} + \mathbf{t}^\dagger s\right) - \frac{i}{2}\,\mathbf{t}^\dagger \times \mathbf{t}.$$

The x-component of the correspondence $\mathbf{S}_j \to \frac{\lambda_j}{2}\left(s^\dagger\mathbf{t} + \mathbf{t}^\dagger s\right)$ was demonstrated in (17) and (18). We recall that we found $S_{1,x}|s\rangle = \frac{1}{2}|t_x\rangle$ whereas $S_{2,x}|s\rangle = -\frac{1}{2}|t_x\rangle$ and the factor of λ_i keeps track of this sign. From the discussion after (17) we see that such a sign – and hence a factor of λ_i – will occur whenever the Hamiltonian induces a transition between states which have opposite parity under $1 \leftrightarrow 2$. The overall form of the terms on the right-hand side follows from the fact that $\mathbf{S}$ is a Hermitean vector operator, so the right-hand side has to be one as well. Indeed, it is easy to verify that the right-hand side is Hermitean, and the vector product $\mathbf{t}^\dagger \times \mathbf{t}$ is the only way to contract two vector operators into a single one. By forming the scalar product, we can now write the exchange term along a bond connecting the sites i and j such that site i belongs to dimer m, site j to dimer n

$$\begin{aligned} J\,\mathbf{S}_i\cdot\mathbf{S}_j \to{}& \frac{J\lambda_i\lambda_j}{4}\left(s^\dagger_m\mathbf{t}_m + \mathbf{t}^\dagger_m s_m\right)\left(s^\dagger_n\mathbf{t}_n + \mathbf{t}^\dagger_n s_n\right) - \frac{J}{4}\,(\mathbf{t}^\dagger_n\times\mathbf{t}_n)\cdot(\mathbf{t}^\dagger_m\times\mathbf{t}_m) \\ &- \frac{iJ}{4}\Big(\lambda_i\left(s^\dagger_m\mathbf{t}_m + \mathbf{t}^\dagger_m s_m\right)\cdot(\mathbf{t}^\dagger_n\times\mathbf{t}_n) + \lambda_j\left(s^\dagger_n\mathbf{t}_n + \mathbf{t}^\dagger_n s_n\right)\cdot(\mathbf{t}^\dagger_m\times\mathbf{t}_m)\Big), \end{aligned} \tag{19}$$

The right-hand side comprises all possible ways to construct a spin scalar from the vectors $\mathbf{t}$ and $\mathbf{t}^\dagger$ and only the numerical prefactors need to be determined. Lastly, using the identity $\varepsilon_{\alpha\beta\gamma}\varepsilon_{\alpha\mu\nu} = \delta_{\beta\mu}\delta_{\gamma\nu} - \delta_{\beta\nu}\delta_{\gamma\mu}$ the double-cross product in (19) can be written as

$$-\frac{J}{4}\,(\mathbf{t}_n^\dagger \times \mathbf{t}_n)\cdot(\mathbf{t}_m^\dagger \times \mathbf{t}_m) = \frac{J}{4}\sum_{\alpha\neq\beta}\left(t_{m,\alpha}^\dagger t_{n,\alpha}\; t_{n,\beta}^\dagger t_{m,\beta} - t_{m,\alpha}^\dagger t_{n,\alpha}^\dagger\; t_{n,\beta} t_{m,\beta}\right). \tag{20}$$

3.2 Spin ladders

Before proceeding with our discussion of the planar model, we make a short digression to *spin ladders* [12, 13]. As one might have expected, these consist of two parallel spin chains – the 'legs' of the ladder – which are coupled by an exchange along the 'rungs' of the ladder, see Figure 11. Such systems can actually be realized in suitably designed copper oxide compounds such as $SrCu_2O_3$ [14]. Here we consider such a ladder with N_r rungs and periodic boundary conditions in x-direction, the exchange constants along the rungs, J_1, and along the legs, J_2, may be different and we assume $J_1 > J_2$. This selects the 'natural' dimer covering in Figure 11(b), because singlets along the rungs give a lower energy than those along the legs. We define the coordinate axes as indicated, whence our convention for assigning the 1-site and 2-site in a dimer gives the λ's as in the Figure. Any two successive rungs m and $m{+}1$ are connected by two bonds, and one of them connects the two 1-sites, the other one the two 2-sites, so that the products $\lambda_i\lambda_j$ in the first term in (19) all are equal to 1. On the other hand, the terms of 3^{rd} order in triplets in the second line of (19) contain only one factor of λ and therefore cancel between the two bonds connecting the rungs m and $m{+}1$. The Hamiltonian becomes [12]

$$\begin{aligned} H = J_1 \sum_m \mathbf{t}_m^\dagger\cdot\mathbf{t}_m + \frac{J_2}{2}\sum_m\left[\left(\mathbf{t}_m^\dagger\cdot\mathbf{t}_{m+1}^\dagger s_m s_{m+1} + H.c\right) + \left(\mathbf{t}_{m+1}^\dagger\cdot\mathbf{t}_m s_{m+1} s_m^\dagger + H.c\right)\right] \\ + \frac{J_2}{2}\sum_{\alpha\neq\beta}\left(t_{m,\alpha}^\dagger t_{m+1,\alpha}\; t_{m+1,\beta}^\dagger t_{m,\beta} - t_{m,\alpha}^\dagger t_{m+1,\alpha}^\dagger\; t_{m+1,\beta} t_{m,\beta}\right) - \frac{3J_1 N_r}{4}. \end{aligned} \tag{21}$$

The first term describes the increase in energy due to replacing a singlet by a triplet and the particles have to obey the constraint $s_m^\dagger s_m + \mathbf{t}_m^\dagger\cdot\mathbf{t}_m = 1$ separately for each rung m. Except for the first one, all terms in this Hamiltonian are 4^{th} order in the Boson operators, so to make any progress we need to make approximations. As a first step, we assume that the singlet Bosons are condensed into the state with momentum $k{=}0$. This implies that all singlet operators $s_m^\dagger$, s_m can be replaced by a real number s, the singlet condensation amplitude. Next, we replace the constraint on particle number for each rung by a single constraint for all rungs

$$N_r s^2 + \sum_m \mathbf{t}_m^\dagger\cdot\mathbf{t}_m - N_r = 0. \tag{22}$$

It needs to be stressed that this approximation is both drastic and questionable: once the $s_m^\dagger$, s_m are replaced by a mere number, the Hamiltonian contains terms such as $\frac{J_2 s^2}{2}\,\mathbf{t}_{m+1}^\dagger\cdot\mathbf{t}_m$, i.e., a free hopping term for the triplets. On the other hand, the original constraint $s_m^\dagger s_m + \mathbf{t}_m^\dagger\cdot\mathbf{t}_m = 1$ implies that at most one triplet can be on any rung – so that the triplets also have to obey a

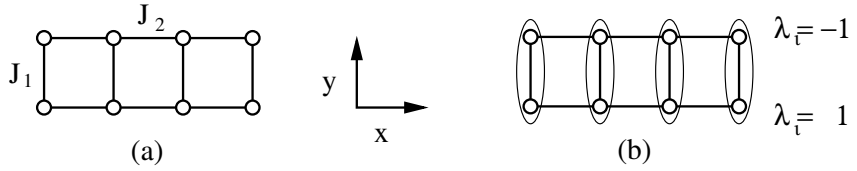

Fig. 11: *A spin ladder.*

hard-core constraint as the magnons. Physically, condensation of the singlets means that they form a kind of inert background and have no excitation spectrum of their own. If this is correct, one might hope that the approximation still is reasonable as long as the density of triplets is low – we made a similar argument for the magnons in linear spin wave theory. Lastly, the terms which are of 4^{th} order in triplet operators are treated in mean-field approximation:

$$\begin{aligned} H_4 &= \frac{J_2}{3}\Big[\Big(\mathbf{t}^\dagger_{m+1}\cdot\mathbf{t}_m\,\langle\mathbf{t}^\dagger_m\cdot\mathbf{t}_{m+1}\rangle - \mathbf{t}^\dagger_m\cdot\mathbf{t}^\dagger_{m+1}\,\langle\mathbf{t}_{m+1}\cdot\mathbf{t}_m\rangle\Big) + H.c.\Big] - A \\ &= J_2\Big[\Big(\,\eta\,\mathbf{t}^\dagger_{m+1}\cdot\mathbf{t}_m - \zeta\,\mathbf{t}^\dagger_m\cdot\mathbf{t}^\dagger_{m+1}\Big) + H.c.\Big] - A. \end{aligned}$$

Here we have introduced the mean-field parameters $\eta = \langle t^\dagger_{m,\alpha}t_{m+1,\alpha}\rangle$ and $\zeta = \langle t_{m+1,\alpha}t_{m,\alpha}\rangle$, which are the same for all α due to spin rotation symmetry, and $A = 3J_2(\eta^2-\zeta^2)$. Lastly, we multiply the constraint (22) by a Lagrange multiplier μ and subtract it from the Hamiltonian. The Hamiltonian is now in a quadratic form and after Fourier transformation becomes

$$\begin{aligned} H_{MF} &= \sum_k \varepsilon_k\,\mathbf{t}^\dagger_k\cdot\mathbf{t}_k + \frac{1}{2}\sum_k \Delta_k\big(\mathbf{t}^\dagger_k\cdot\mathbf{t}^\dagger_{-k} + H.c\big) - n_rA - \mu N_r(s^2{-}1) \\ &= \sum_{k>0}\Big(\varepsilon_k\,(\mathbf{t}^\dagger_k\cdot\mathbf{t}_k + \mathbf{t}^\dagger_{-k}\cdot\mathbf{t}_{-k}) + \Delta_k\,(\mathbf{t}^\dagger_k\cdot\mathbf{t}^\dagger_{-k} + \mathbf{t}_{-k}\cdot\mathbf{t}_k)\Big) - N_rA - \mu N_r(s^2{-}1), \\ \varepsilon_k &= J_1 + J_2\big(s^2{+}2\eta\big)\cos(k) - \mu, \qquad \Delta_k = J_2\big(s^2{-}2\zeta\big)\cos(k). \end{aligned} \tag{23}$$

Note that the Lagrange multiplier μ appears in both, the additive constant and the term ε_k where it may be viewed to act as an additive renormalization $J_1 \to J_1{-}\mu$ of the energy of formation of a triplet. Each of the blocks for a given $k > 0$ can be diagonalized by the ansatz

$$\begin{array}{rcl} \boldsymbol{\tau}^\dagger_k &=& u_k\mathbf{t}^\dagger_k + v_k\mathbf{t}_{-k} \\ \boldsymbol{\tau}_{-k} &=& v_k\mathbf{t}^\dagger_k + u_k\mathbf{t}_{-k} \end{array} \quad\Rightarrow\quad \begin{array}{rcl} \mathbf{t}^\dagger_k &=& u_k\boldsymbol{\tau}^\dagger_k - v_k\boldsymbol{\tau}_{-k} \\ \mathbf{t}_{-k} &=& -v_k\boldsymbol{\tau}^\dagger_k + u_k\boldsymbol{\tau}_{-k} \end{array} \tag{24}$$

where again $u_k^2{-}v_k^2 = 1$. The requirement $[H,\tau^\dagger_{k,\nu}] = \omega_k\tau^\dagger_{k,\nu}$ again leads to a $2{\times}2$ eigenvalue problem and we obtain

$$\omega_k \;=\; \sqrt{\varepsilon_k^2 - \Delta_k^2}, \qquad u_k = \frac{\Delta_k}{\sqrt{2\omega_k(\varepsilon_k-\omega_k)}}, \qquad v_k = \sqrt{\frac{\varepsilon_k-\omega_k}{2\omega_k}}. \tag{25}$$

Reinserting (24) into H_{MF} one finds after a somewhat lengthy calculation that

$$H_{MF} = \sum_{k>0}\Big(\omega_k(\boldsymbol{\tau}^\dagger_k\cdot\boldsymbol{\tau}_k + \boldsymbol{\tau}^\dagger_{-k}\cdot\boldsymbol{\tau}_{-k}) + 3(\omega_k-\varepsilon_k)\Big) - 3N_rJ_2(\eta^2-\zeta^2) - \mu N_r(s^2-1).$$

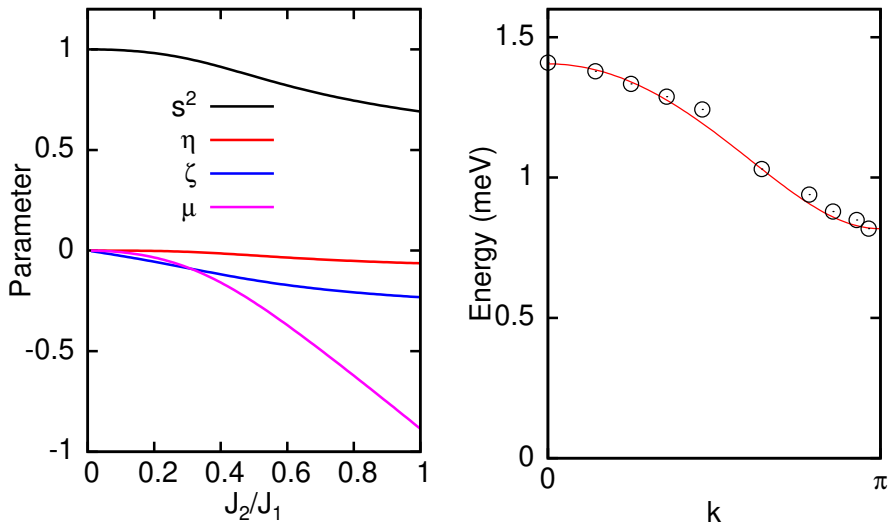

Fig. 12: *Left: mean-field parameters obtained by self-consistent solution of the system of equations (26) as functions of J_2/J_1 [13]. Right: triplet dispersion ω_k in (25) calculated self-consistently for $J_1 = 1.09\,meV$ and $J_2 = 0.30\,meV$ compared to the experimental dispersion for the spin ladder compound $(C_5D_{12}N)_2CuBr_4$ [16].*

It remains to determine the singlet condensation amplitude s, the mean-field parameters η and ζ, and the Lagrange multiplier μ. We consider s, η and ζ as freely adjustable parameters in the Hamiltonian, whence a well-known theorem from thermodynamics [15] tells us that these parameters will adjust themselves such as to minimize the Helmholtz Free Energy $F = U - T{\cdot}S$ of the system. The same holds true for the Lagrange multiplier μ. We restrict ourselves to the case of zero temperature, where $F = U$, the expectation value of H_{MF} in its ground state. The ground state is the vacuum for the $\boldsymbol{\tau}^\dagger$-Bosons, so we can drop the terms $(\boldsymbol{\tau}_k^\dagger \cdot \boldsymbol{\tau}_k + \boldsymbol{\tau}_{-k}^\dagger \cdot \boldsymbol{\tau}_{-k})$ and find

$$U = \frac{3}{2}\sum_k (\omega_k - \varepsilon_k) - 3N_r J_2(\eta^2 - \zeta^2) - \mu N_r(s^2 - 1).$$

Setting the derivatives with respect to the four parameters equal to zero we find

$$\begin{aligned} s^2 &= 1 - \frac{3}{N}\sum_k \frac{\varepsilon_k - \omega_k}{2\omega_k}, & \mu &= \frac{3J_2}{N}\sum_k \frac{\varepsilon_k - \omega_k - \omega_k}{2\omega_k}\cos(k), \\ \eta &= \frac{1}{N}\sum_k \frac{\varepsilon_k - \omega_k}{2\omega_k}\cos(k), & \zeta &= -\frac{1}{N}\sum_k \frac{\Delta_k}{2\omega_k}\cos(k). \end{aligned} \tag{26}$$

This set of self-consistency equations can be solved numerically and the results are shown in Figure 12. We note that s^2 is close to unity, and Eq. (22) then tells us that the density of triplets is low so that the majority of rungs is in the singlet state. The Lagrange multiplier μ is large and negative. As stated above, μ may be considered as an additive correction to the triplet energy $J_{1,eff} = J_1 + |\mu|$. Apparently J_1 is enhanced considerably: due to the hard-core constraint, presence of a triplet on rung m blocks this rung, that means no other triplets can be created on this rung and no other triplet can hop to this rung. It follows that there will be a loss of kinetic energy $\propto J_2$ of the triplets, and this has to be added to the energy cost J_1 for adding a triplet to the system. Consistent with this interpretation, this correction becomes

more important for larger J_2. Finally, the mean-field parameters η and ζ are rather small and could be neglected – this is a consequence of the low density of triplets, $1-s^2$. Figure 12 also shows a comparison of the mean-field dispersion ω_k to the experimental dispersion obtained by INS for the compound $(C_5D_{12}N)_2CuBr_4$, in which the Cu^{2+} ions indeed form spin ladders [16]. With the choice $J_1 = 1.09\,\text{meV}$ and $J_2 = 0.30\,\text{meV}$ the mean-field theory gives quite a good description of experiment, but it should be noted that for other compounds where J_2/J_1 is closer to one the agreement is less satisfactory.

3.3 Planar system

We now return to the planar system and first restrict ourselves to a pure spin system without holes. As we have seen above, the ground state of the half-filled system has antiferromagnetic order and is well described by spin wave theory, so considering the planar Heisenberg model without antiferromagnetic order is strictly speaking unphysical. However, we continue the discussion of the singlet soup because we want to construct a theory for a disordered spin state and its excitations, so as to set the stage for adding the mobile holes. In exactly the same way as for spin ladders we can use the expressions (19) for the Heisenberg exchange to rewrite the Heisenberg Hamiltonian *exactly* in terms of the singlets and triplets for any given dimer covering of the plane such as in Figure 10(a). On the other hand we do not gain very much in this way, because even writing down a dimer covering for a macroscopic system is not feasible, let alone solve the corresponding Hamiltonian. One might consider choosing a particular 'simple' dimer covering, such as periodically repeating the spin ladder in Figure 11 in y-direction. However, since one is forced to make approximations, the special symmetry of the covering will make itself felt in the approximate solutions as an artificial supercell structure, leading to a reduction of the Brillouin zone and an unphysical backfolding of bands.

On the other hand, rewriting the Hamiltonian in terms of the singlet and triplet Bosons provides an exact representation of the Heisenberg model for *any* dimer covering of the plane. This means that, for example, the result for the spin correlation function $\langle \mathbf{S}_j(t) \cdot \mathbf{S}_i \rangle$ cannot depend on the specific dimer covering in which the calculation is carried out. Put another way, the way in which a spin excitation propagates through the network of dimers from site $i \to j$ during the time t does not depend at all on the geometry of the particular dimer covering. This suggests to construct a translationally invariant approximate Hamiltonian by *averaging* the dimer Hamiltonian over all possible coverings.This means that now *every* bond in the lattice may be occupied by a Boson and the averaged Hamiltonian for two bonds m and n connected by the exchange term is $\bar{h}_{m,n} = \zeta\, h_{m,n}$ with $h_{m,n}$ given in (19) and

$$\zeta = \frac{N_{m,n}}{N_d}. \tag{27}$$

Here $N_{m,n}$ is the number of dimer coverings which contain the bonds n and m whereas N_d is the total number of dimer coverings. The resulting Hamiltonian obviously is translationally invariant and isotropic. We estimate ζ by a crude approximation: consider two adjacent bonds

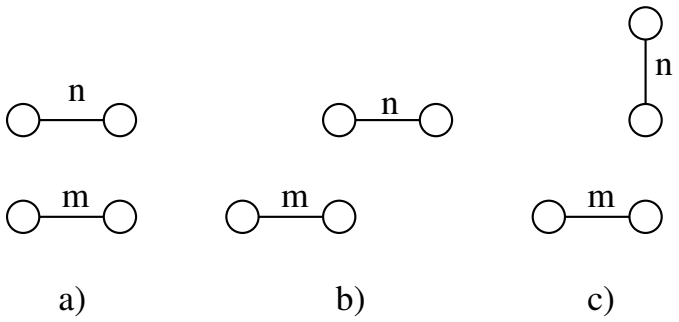

Fig. 13: *Estimation of the renormalization factor ζ.*

as in Figure 13. By symmetry the bond m is covered by a dimer in exactly $1/4$ of all dimer coverings and we restrict ourselves to these. Assuming for simplicity that the number of coverings containing one of the three possible orientations of the adjacent bond n are equal, we estimate $\zeta = 1/12$. From now on, we proceed in the same way as in the case of spin ladders. As a first step we assume that the singlets are condensed and replace all operators $s_m^\dagger$, s_m in (19) by a real number s. To keep things simple we, moreover, discard the interaction terms in (19), that means the terms of 3^{rd} or 4^{th} order in the triplet operators. The terms of 4^{th} order could again be treated in mean-field approximation but as we have seen in the discussion of spin ladders the corresponding mean-field parameters η and ζ were quite small. With these simplifications the Hamiltonian becomes

$$H = \tilde{J} \sum_m \mathbf{t}_m^\dagger \cdot \mathbf{t}_m^\dagger + \frac{\zeta s^2}{4} \sum_{m,n} \sum_{\substack{i \in m \\ j \in n}} J_{i,j}\, \lambda_i\, \lambda_j \Big(\mathbf{t}_m^\dagger \cdot \mathbf{t}_n^\dagger + \mathbf{t}_n \cdot \mathbf{t}_m + \mathbf{t}_m^\dagger \cdot \mathbf{t}_n + \mathbf{t}_n^\dagger \cdot \mathbf{t}_m \Big). \qquad (28)$$

The sum runs over all $2N$ bonds in the averaged system, $J_{i,j} = J$ when i and j are nearest neighbors and zero otherwise. The first term describes the change in energy when a singlet on bond m is replaced by a triplet, and initially we set $\tilde{J} = J$. The second term describes the propagation of the triplets. Being a quadratic form, (28) is readily diagonalized by Fourier transform – we only need to specify a convention for the position of a bond: if bond m connects the sites i and j we define $\mathbf{R}_m = (\mathbf{R}_i + \mathbf{R}_j)/2$. Moreover we have to keep in mind that we have two species of bonds, namely bonds in x-directions and bonds in y-direction. We specify this by an additional subscript for the Fourier transformed operators, e.g., $\mathbf{t}_{\mathbf{k},\mu}^\dagger$ with $\mu \in \{x, y\}$. The products $\lambda_i \lambda_j$ are given in Figure 14 from which we readily can read off

$$H = \sum_{\mathbf{k}} \sum_{\mu,\mu' \in \{x,y\}} \left(\mathbf{t}_{\mathbf{k},\mu}^\dagger \left(\tilde{J} \delta_{\mu\mu'} + \varepsilon_{\mu,\mu'}(\mathbf{k}) \right) \mathbf{t}_{\mathbf{k},\mu'} + \frac{1}{2} \left(\mathbf{t}_{\mathbf{k},\mu}^\dagger\, \varepsilon_{\mu,\mu'}(\mathbf{k})\, \mathbf{t}_{-\mathbf{k},\mu'}^\dagger + H.c. \right) \right)$$

with

$$\begin{aligned} \varepsilon_{x,x}(\mathbf{k}) &= \zeta s^2 J \left(\cos(k_y) - \frac{1}{2}\cos(2k_x) - \cos(k_x)\cos(k_y) \right), \\ \varepsilon_{x,y}(\mathbf{k}) &= \zeta s^2 J \left(\sin\Big(\frac{3k_x}{2}\Big) \sin\Big(\frac{k_y}{2}\Big) + \sin\Big(\frac{k_x}{2}\Big) \sin\Big(\frac{3k_y}{2}\Big) \right), \end{aligned}$$

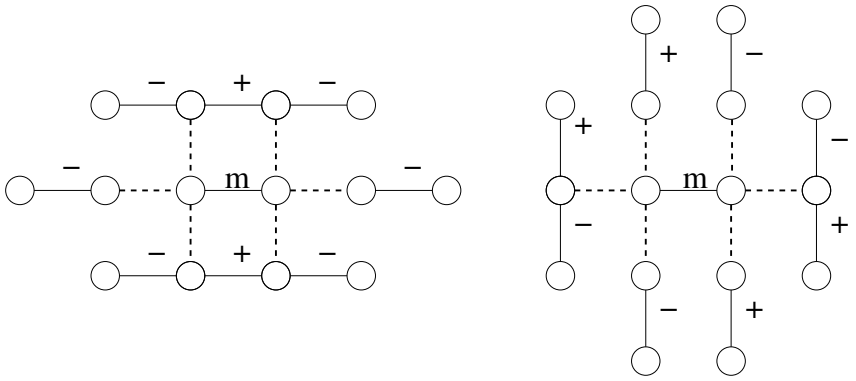

Fig. 14: *The factors of $\lambda_i\lambda_j$ for all bonds connected to the bond m by a nearest neighbor bond. In a) both bonds are along the x-direction so that these pairs contribute to $\varepsilon_{x,x}$ whereas in b) one bond is along y-direction so that these pairs contribute to $\varepsilon_{x,y}$. In a) both bonds connecting parallel bonds have $\lambda_i\lambda_j = 1$.*

$\varepsilon_{y,x} = \varepsilon_{x,y}$, and $\varepsilon_{y,y}$ is obtained from $\varepsilon_{x,x}$ by $k_x \leftrightarrow k_y$. To diagonalize H we repeat the procedure for spin ladders and make the *ansatz* (with $\nu \in \{1,2\}$)

$$\begin{aligned} \boldsymbol{\tau}^\dagger_{\nu,\mathbf{k}} &= \sum_{\mu\in\{x,y\}} \left(u_{\nu,\mathbf{k},\mu}\, \mathbf{t}^\dagger_{\mathbf{k},\mu} + v_{\nu,\mathbf{k},\mu}\, \mathbf{t}_{-\mathbf{k},\mu} \right), \\ \boldsymbol{\tau}_{\nu,-\mathbf{k}} &= \sum_{\mu\in\{x,y\}} \left(v^*_{\nu,\mathbf{k},\mu}\, \mathbf{t}^\dagger_{\mathbf{k},\mu} + u^*_{\nu,\mathbf{k},\mu}\, \mathbf{t}_{-\mathbf{k},\mu} \right), \end{aligned} \tag{29}$$

Demanding $[H,\, \boldsymbol{\tau}^\dagger_{\nu,\mathbf{k}}] = \omega_{\nu,\mathbf{k}} \boldsymbol{\tau}^\dagger_{\nu,\mathbf{k}}$ gives the non-Hermitean 4×4 eigenvalue problem

$$\begin{pmatrix} \tilde{J}+\varepsilon_{\mathbf{k}} & -\varepsilon_{\mathbf{k}} \\ \varepsilon^*_{-\mathbf{k}} & -\tilde{J}-\varepsilon^*_{-\mathbf{k}} \end{pmatrix} \begin{pmatrix} u_{\nu,\boldsymbol{k}} \\ v_{\nu,\boldsymbol{k}} \end{pmatrix} = \omega_{\nu,\mathbf{k}} \begin{pmatrix} u_{\nu,\boldsymbol{k}} \\ v_{\nu,\boldsymbol{k}} \end{pmatrix}. \tag{30}$$

For a matrix like the one on the left hand side it is easy to show that if (u, v) is an eigenvector with eigenvalue ω, then (v^*, u^*) is an eigenvector with eigenvalue $-\omega$ so that the eigenvalues come in pairs of $\pm\omega$. We multiply (30) by $\omega_{\nu,\mathbf{k}}$ and replace products such as $\omega_{\nu,\mathbf{k}} u_{\nu,\boldsymbol{k}}$ or $\omega_{\nu,\mathbf{k}} v_{\nu,\boldsymbol{k}}$ on the left hand side of the resulting equations by the expressions given by the original version of (30). Since the commutator $[\tilde{J}+\varepsilon_{\mathbf{k}},\, \varepsilon_{\mathbf{k}}] = 0$ we obtain

$$\left(\tilde{J}^2 + 2\tilde{J}\varepsilon_{\mathbf{k}}\right) u_{\nu,\boldsymbol{k}} = \omega^2_{\nu,\mathbf{k}}\, u_{\nu,\boldsymbol{k}},$$

and the same equation for $v_{\nu,\boldsymbol{k}}$. It follows that $\omega_{\nu,\mathbf{k}} = \sqrt{\tilde{J}^2 + 2\tilde{J}\lambda_{\nu,\mathbf{k}}}$, where $\lambda_{\nu,\mathbf{k}}$ are the eigenvalues of the Hermitean 2×2 matrix $\varepsilon_{\mathbf{k}}$, and both, $u_{\nu,\boldsymbol{k}}$ and $v_{\nu,\boldsymbol{k}}$, must be the corresponding eigenvector, albeit multiplied by different prefactors. The eigenvalues of $\varepsilon_{\mathbf{k}}$ are $\lambda_{1,\mathbf{k}} = -\zeta s^2 J/2$ and $\lambda_{2,\mathbf{k}} = \zeta s^2 J(3/2 + 2\gamma_{\mathbf{k}} - 4\gamma^2_{\mathbf{k}})$, with $\gamma_{\mathbf{k}}$ given in (5).

In principle we should now repeat the self-consistency procedure for spin ladders but for the sake of simplicity we switch to a more phenomenological description, using the discussion of spin ladders as a guideline. There we saw that the energy needed to convert a singlet into a

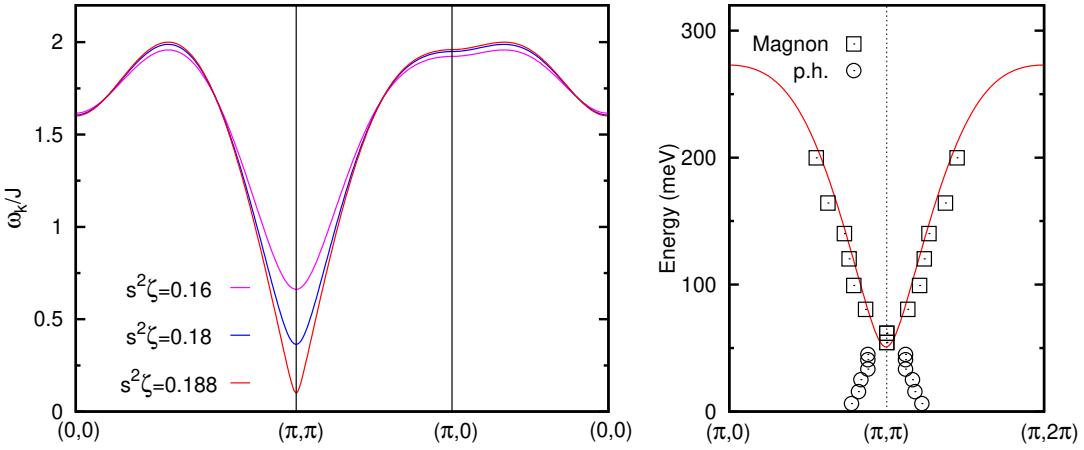

Fig. 15: *Left: Spin excitation dispersion relation $\omega_{\mathbf{k}}$ using the parameter values $\tilde{J} = 1.7\,J$ and different $s^2\zeta$. Right: $\omega_{\mathbf{k}}$ calculated for $\tilde{J} = 1.7\,J$, $s^2\zeta = 0.16$ and $J = 140\,meV$ compared to the hourglass dispersion measured in $La_{1.875}Ba_{0.125}CuO_4$ [17]. The data points labeled 'Magnon' correspond to the triplet dispersion, the points labeled 'p.h.' correspond to particle-hole excitations which are absent in our theory.*

triplet was increased to $J_1+|\mu|$ – see (23) – whereby $|\mu|$ could be quite appreciable for $J_2 \to J_1$, see Figure 12. We had interpreted this as an additional cost in kinetic energy because a triplet would block a given rung. Clearly the same would happen also for the planar system, and accordingly we assume that the prefactor of the first term in (28) is $\tilde{J} > J$ which we take as a first adjustable parameter. Next, we will not attempt to calculate the singlet condensation amplitude s but consider the product $s^2\zeta$ as a single adjustable parameter. We recall that ζ was determined somewhat vaguely anyway. Our theory now has two adjustable parameters, which we use to fix two physical quantities, the total bandwidth of the spin excitations, and the spin gap (to be explained below). Lastly, we recall that we have two eigenvalues $\lambda_{\nu,\mathbf{k}}$ for each wave vector $\mathbf{k}$, whereby $\lambda_{1,\mathbf{k}}$ has the peculiar feature of being independent of $\mathbf{k}$. A more detailed analysis shows [18], that the band derived from the dispersionless eigenvalue also has zero spectral weight in the spin correlation function. This suggests, that this band is an artifact of the enlargement of the basis by doubling the number of bonds. We therefore drop this dispersionless band and retain only the band of spin excitations resulting from $\lambda_{2,\mathbf{k}}$. Figure 15 then shows the resulting triplet dispersion $\omega_{\mathbf{k}}$. The parameter $\tilde{J}$ has been adjusted to set the total bandwidth to $2J$, the bandwidth for antiferromagnetic spin waves. $\omega_{\mathbf{k}}$ has its minimum at (π,π) and the energy at this wave vector is frequently called the spin gap, Δ_S. With increasing value of $s^2\zeta$, Δ_S closes rapidly and one can envisage how for $\Delta_S \to 0$ the cone-shaped dispersion of antiferromagnetic spin waves at (π,π) is recovered. Experimentally, INS on many cuprate compounds shows an 'hourglass' dispersion around (π,π) – an example is shown in Figure 15. This is frequently interpreted [19] as a magnon-like collective mode above the neck of the hour-glass co-existing with particle-hole excitations of the Fermi gas of free carriers below the neck. The part above the neck of the hourglass thus should correspond to our triplet band and the comparison in Figure 15 shows reasonable agreement.

3.4 Doped holes

Having developed a description for a disordered spin system we are finally ready to include doped holes into our theory. To that end we introduce dimers which contain a single electron or no electron at all. We again consider a dimer with sites 1 and 2, but now assume that the dimer contains one electron with spin σ. This means that instead of the exchange term now the hopping term is active: $H_t = -t\sum_\sigma \left(\hat{c}^\dagger_{1,\sigma}\hat{c}_{2,\sigma} + H.c.\right)$ and there are two eigenstates of H_t

$$|f_{\pm,\sigma}\rangle = \frac{1}{\sqrt{2}}\Big(\hat{c}^\dagger_{1,\sigma} \pm \hat{c}^\dagger_{2,\sigma}\Big)|0\rangle, \tag{31}$$

which obviously obey $H_t|f_{\pm,\sigma}\rangle = \mp t|f_{\pm,\sigma}\rangle$. To extend our theory to doped system, we introduce a new type of effective particle to represent dimers occupied by one electron. Namely if dimer m is in one of the states $|f_{\pm,\sigma}\rangle$ we consider it as occupied by a Fermion, created by $f^\dagger_{m,\pm,\sigma}$. We choose a Fermion, because the number of electrons in such a dimer is one. We also introduce one more Boson, created by $e^\dagger$, to represent an empty dimer. In order to include these particles we need to transcribe the electron creation and annihilation operators $\hat{c}^\dagger_{i,\sigma}$ and $\hat{c}_{i,\sigma}$. The two spin components of any Fermion creation operator can be combined into a two-component vector or spinor $\mathbf{a}^\dagger = \left(a^\dagger_\uparrow, a^\dagger_\downarrow\right)^T$. The spin components of any Fermion annihilation operator also can be combined into a spinor $\mathbf{a} = \left(a_\uparrow, a_\downarrow\right)^T$ but under spin rotations this type of spinor transforms as $i\tau_y\mathbf{a}^\dagger$ [20]. Using this notation we can write (with $j \in \{1,2\}$)

$$\mathbf{c}_j \to :\ \frac{1}{2}\big(s\, i\tau_y + \lambda_j \mathbf{t}\cdot\boldsymbol{\tau} i\tau_y\big)\left(\mathbf{f}^\dagger_+ - \lambda_j \mathbf{f}^\dagger_-\right) + \frac{1}{\sqrt{2}}\, e^\dagger\left(\mathbf{f}_+ + \lambda_j \mathbf{f}_-\right)\ : \tag{32}$$

where $: \cdots :$ denotes normal ordering. As was the case for the triplets, the overall form of the terms on the right-hand side can be guessed by making use of the transformation properties under spin rotations. Namely the 'spinor product' $\mathbf{t}\cdot\boldsymbol{\tau}\mathbf{a}$ is the way to construct a new spinor from a vector operator $\mathbf{t}$ and given spinor $\mathbf{a}$. The factors of λ_j again are associated with states of opposite parity under $1 \leftrightarrow 2$. From now on we omit the terms involving the $e^\dagger$-Bosons because for low hole concentration the probability to find two holes in the same dimer will be small. We rewrite the hopping term, again along a bond connecting the sites i and j such that site i belongs to dimer m, site j to dimer n:

$$\begin{aligned} -t\sum_\sigma \hat{c}^\dagger_{i,\sigma}\hat{c}_{j,\sigma} \to\ & \frac{t}{4}\Big((s^\dagger_m s_n\ + \lambda_i\lambda_j \mathbf{t}^\dagger_m\cdot\mathbf{t}_n)\Big(\sum_\sigma f^\dagger_{n,j,\sigma} f_{m,i,\sigma}\Big) \\ & - \big(\lambda_i \mathbf{t}^\dagger_m s_n + \lambda_j s^\dagger_m \mathbf{t}_n\big)\cdot\mathbf{v}_{(n,j),(m,i)} - i\lambda_i\lambda_j\big(\mathbf{t}^\dagger_m\times\mathbf{t}_n\big)\cdot\mathbf{v}_{(n,j),(m,i)}\Big), \end{aligned} \tag{33}$$

where the combination $f_{m,i,\sigma} = f_{m,+,\sigma} - \lambda_i\, f_{m,-,\sigma}$ and the vector

$$\mathbf{v}_{(n,j),(m,i)} = \sum_{\sigma,\sigma'} f^\dagger_{n,j,\sigma}\,\boldsymbol{\tau}_{\sigma,\sigma'}\, f_{m,i,\sigma'}$$

obeys $[S_\alpha,\, v_\beta] = i\varepsilon_{\alpha\beta\gamma}\, v_\gamma$. Again, the right-hand side is a linear combination of all possible ways to construct a spinor from another spinor and one or two vector operators. Next, we make

analogous approximations as in the case of the triplet Hamiltonian. We average the Hamiltonian over dimer coverings, again introducing the factors of ζ. We discard the terms in the second line of (33) which describe the emission/absorption of a triplet by a Fermion or the scattering of a Fermion from a triplet. The terms in the first line of (33) are treated in mean-field approximation, that means we replace the singlet operators $s_m^\dagger$, s_m by the real number s, the singlet condensation amplitude. A full mean-field decomposition would also produce expectation values such as $\langle \mathbf{t}_m^\dagger \cdot \mathbf{t}_m \rangle$, but such expectation values were discarded above and we do the same here. All in all we obtain in this way

$$H_F = -t \sum_{m,\sigma} \left(f_{m,+,\sigma}^\dagger f_{m,+,\sigma} - f_{m,-,\sigma}^\dagger f_{m,-,\sigma} \right) + \frac{s^2 \zeta t}{4} \sum_{m,n} \sum_{\substack{i \in m \\ j \in n}} \sum_{\sigma} f_{n,j,\sigma}^\dagger f_{m,i,\sigma}, \qquad (34)$$

where the sums over m and n run over all $2N$ bonds in the system.

We now arrive at the crucial point which distinguishes the present theory from most others: how do we count the electrons? Obviously, each $f_{m,\pm,\sigma}^\dagger$-Fermion contains one hole and has a z-spin of σ. Accordingly, in a given dimer covering the number of Fermions must be equal to the number of doped holes, $N_h = N - N_e$

$$N_h = \sum_{m,\sigma} \left(f_{m,+,\sigma}^\dagger f_{m,+,\sigma} + f_{m,-,\sigma}^\dagger f_{m,-,\sigma} \right), \qquad (35)$$

where the sum is over the $N/2$ dimers. We have obtained an approximate theory by averaging over dimer coverings, so that each of the $2N$ bonds in the plane can be occupied by a Boson or Fermion. The physically relevant quantity, however, is the *density of holes per site*, whereas the number of dimers looses its significance due to the averaging approximation. We therefore retain the condition (35), but with the sum over m now over all $2N$ bonds in the system. This condition implies, that the bands obtained by diagonalizing (34) have to be filled from below with N_h *holes*, and since the $f_{m,\pm,\sigma}^\dagger$-Fermions have a spin of $\frac{1}{2}$, the Fermi surface covers a fraction of $n_h/2$ of the Brillouin zone. As the Mott-insulator is approached, $n_e \to 1$ or $n_h \to 0$, the volume of the Fermi surface approaches zero.

We continue with the discussion of the band structure. We are interested mainly in the lowermost bands – these are the ones which will accommodate the doped holes – so for simplicity we drop the $f_{m,-,\sigma}^\dagger$-Fermions, because their energy is $2t$ above that of the $f_{m,+,\sigma}^\dagger$-Fermions, whereas the dispersive terms are $\propto s^2\zeta t \approx 0.2t$. With this last approximation Fourier transformation gives $H_F = \sum_{\mathbf{k},\sigma} v_{\mathbf{k},\sigma}^\dagger \tilde{H}_{\mathbf{k}} v_{\mathbf{k},\sigma}$ with the vector $v_{\mathbf{k},\sigma} = (f_{\boldsymbol{k},x,+,\sigma}, f_{\boldsymbol{k},y,+,\sigma})^T$. The $\mathbf{k}$-dependence of the 2×2 matrix $\tilde{H}_{\mathbf{k}}$ can again be read off from Figure 14, but with all $\lambda = 1$. We obtain

$$\tilde{H}_{x,x} = -t + s^2\zeta t \left(\cos(k_y) + \cos(k_x)\cos(k_y) + \frac{1}{2}\cos(2k_x) \right)$$
$$\tilde{H}_{x,y} = s^2\zeta t \left(\cos\Big(\frac{3k_x}{2}\Big)\cos\Big(\frac{k_y}{2}\Big) + \cos\Big(\frac{k_x}{2}\Big)\cos\Big(\frac{3k_y}{2}\Big) \right),$$

$\tilde{H}_{y,x} = \tilde{H}_{x,y}$ and $\tilde{H}_{y,y}$ is obtained from $\tilde{H}_{x,x}$ by $k_x \leftrightarrow k_y$. The eigenvalues of $\tilde{H}_{\mathbf{k}}$ are $\varepsilon_{1,\mathbf{k}} = -t + s^2\zeta t/2$ and $\varepsilon_{2,\mathbf{k}} = -t + s^2\zeta t(-3/2 + 2\gamma_{\mathbf{k}} + 4\gamma_{\mathbf{k}}^2)$. More detailed investigation shows [18]

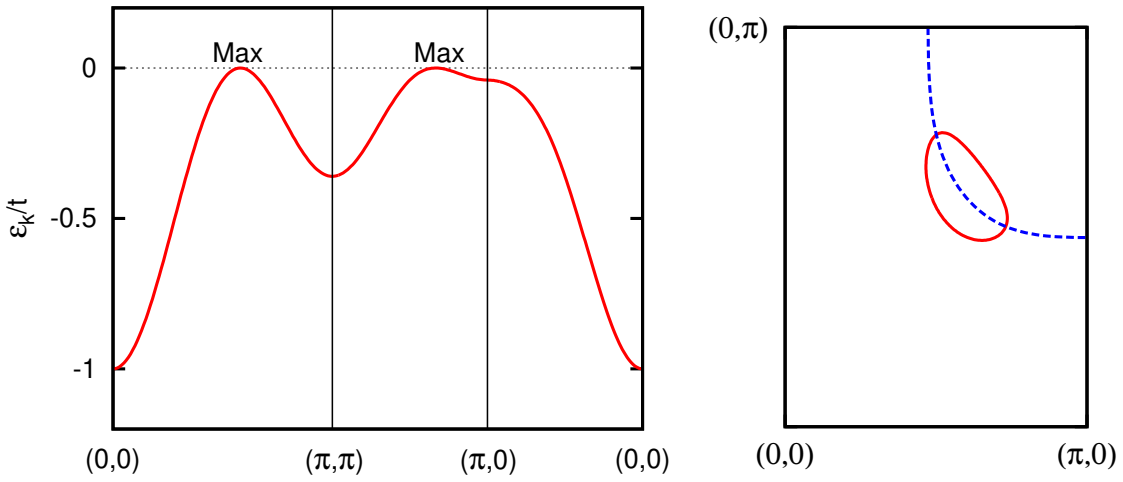

Fig. 16: *Left: Dispersion dispersion relation $-\varepsilon_{2,\boldsymbol{k}}$ for $s^2\zeta = 0.16$. Holes would occupy the maxima of this band – indicated in the Figure – so that the zero of energy corresponds roughly to the Fermi energy for small doping. Right: Adding additional hopping terms between $(1,1)$ and $(2,0)$-like neighbors lifts the degeneracy of the band maximum (indicated in blue) and the Fermi surface takes the form of a hole pocket (indicated in red) [18]. The values are $t' = -0.2t$, $t'' = 0.1t$ and the hole concentration $\delta = 1-n_e = 0.1$.*

that the dispersionless band $\varepsilon_{1,\mathbf{k}}$ has zero weight in the electron spectral function, so again we interpret this as an artifact of the enlargement of the basis states and discard it. As we have seen above the band structure resulting from (34) has to be filled with holes from below, that means at $T = 0$ the condition for the Fermi energy E_F is

$$n_h = \frac{2}{N}\sum_{\boldsymbol{k}} \Theta\big(\varepsilon_{2,\mathbf{k}} - E_F\big).$$

Figure 16 shows $-\varepsilon_{2,\mathbf{k}}$, that means the band is again turned upside down as it would be seen in ARPES. The maxima therefore correspond to the minima of $\varepsilon_{2,\mathbf{k}}$, and this is the location in $\mathbf{k}$-space where the doped holes would accumulate. $\varepsilon_{2,\mathbf{k}}$ depends on $\mathbf{k}$ only via $\gamma_{\mathbf{k}}$, so that lines of constant $\gamma_{\mathbf{k}}$ automatically are lines of constant $\varepsilon_{2,\mathbf{k}}$, in particular the maximum of the inverted dispersion is a roughly circular contour around (π,π). The Fermi surface therefore would be a ring with a width $\propto n_h$, which does not agree with ARPES results. This is a drawback of the present approximation and it is likely that even a small perturbation would lift the degeneracy of the maximum and lead to a unique maximum around which the Fermi surface would be centered. One such perturbation could be the additional hopping terms $\propto t', t''$ discussed above and inclusion of the terms indeed lifts the degeneracy and leads to a Fermi surface which takes the form of a hole pocket centered along the $(1,1)$ direction, see Fig. 16. Comparing to experiment, the pocket is shifted towards (π,π) – one might speculate that including the coupling between holes and triplets, described by the omitted terms in (33) might improve this, but at present this is speculation.

4 Summary and outlook

As explained in the introduction, the hallmark of a Mott insulator is the breakdown of the Fermi surface due to the effectively enhanced Coulomb repulsion in 'small' atomic orbitals: if the number of electrons is equal to the number of sites, N, the electrons are caught in a 'traffic jam' and form a spin system instead of a half-filled band with a Fermi surface. The spins interact via virtual hopping processes of electrons as described by the Heisenberg exchange, which leads to antiferromagnetic correlations and spin excitations.

In the description of the *doped* Mott insulator given in the preceding sections, the electrons continue to form a mere spin system: the majority of electrons are coupled to inert ('condensed') singlets, a few singlets are excited to the triplet state, so that most electrons still contribute only their spin degrees of freedom. This is not surprising, because for a low density of vacancies, most electrons still are completely surrounded by other electrons and thus 'stuck'. Instead, the true mobile Fermions in the system are the $f^\dagger$-particles, which may be viewed as tightly bound states of a spinless hole and one spin, and their number equals the doped holes. Since the $f^\dagger$-particles have a spin of $\frac{1}{2}$, their Fermi surface covers a fraction $n_h/2$ of the Brillouin zone, where $n_h = 1-n_e$ is the concentration of *holes*. We recall that for free electrons the fraction of the Brillouin zone covered by the Fermi surface is $n_e/2$, which differs drastically from $n_h/2$.

On the other hand, the state where the electrons are 'jammed' and form an inert background can persist only over a limited range of the hole concentration n_h. A crude estimate for the range of stability of this phase can be obtained by noting that once the hole concentration reaches $1/z = 0.25$, on average each electron will find an empty site on one of its z neighbors to which it can hop without creating a double occupancy. With increasing n_h it therefore will become energetically favorable for the electrons to form the all-electron Fermi surface of the free electron gas, although the strong scattering will lead to correlation narrowing of the quasiparticle band and strong incoherent weight in the single-particle spectral function. In fact, in the limit $n_e \to 0$ it is known [5] that one recovers a Fermi surface with volume $n_e/2$ but enhanced effective mass.

Accordingly, at some critical hole concentration $n_{h,c}$ we expect a phase transition from the doped Mott-insulator with a hole-like Fermi surface of fractional volume $n_h/2$ described by the above theory, to a renormalized all-electron Fermi liquid with an electron-like Fermi surface of fractional volume $n_e/2$. And, in fact, the experimental situation has pretty much converged to this scenario: a transition between two nonmagnetic Fermi liquids of spin-$\frac{1}{2}$ particles without any obvious order but different Fermi surface volume, which occurs at a hole concentration $n_{h,c} \approx 0.22$. This is discussed in detail in Ref. [18]. Assuming that this $T = 0$ phase transition 'shrouds itself in superconductivity' as quantum phase transitions often do, one arrives at the phase diagram in Figure 17. In fact, unlike many other quantum phase transitions, the transition in the cuprates appears to be between two phases which are homogeneous, isotropic and nonmagnetic and differ only in the Fermi surface volume, so that there is no obvious order parameter. This would be consistent with the above scenario. The detailed description of this transition and how it can give rise to the spectacularly high superconducting transition temperatures is probably the key problem in understanding cuprate superconductors.

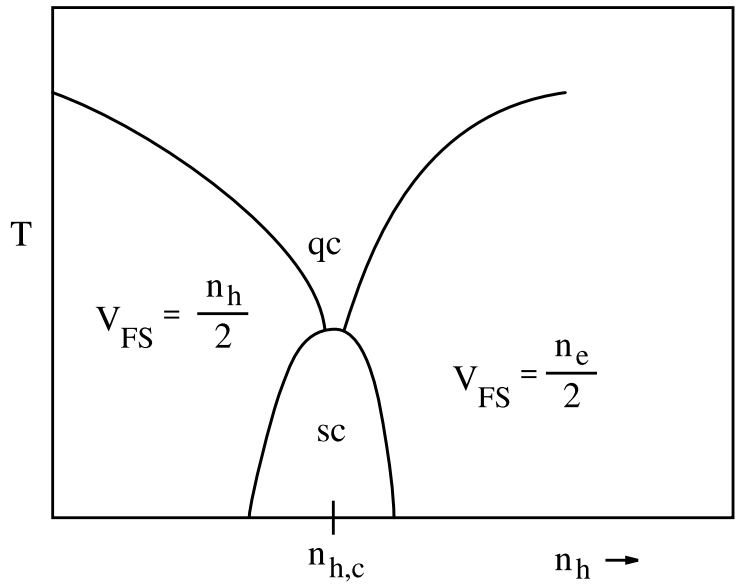

Fig. 17: *Schematic phase diagram for the cuprate superconductors. There is a quantum critical point at the hole concentration $n_{h,c} \approx 0.22$ which at $T = 0$ corresponds to a transition between two Fermi liquids of different fractional Fermi surface volume V_{FS}. The transition gives rise to a superconducting dome (sc) in the phase diagram, and a quantum critical region with non-Fermi liquid behavior above it (qc).*

References

[1] J.G. Bednorz and K.A. Müller, Z. Phys. B **64**, 189 (1986)

[2] K.A. Chao, J. Spałek, A.M. Oleś, J. Phys. C10, L **271** (1977)

[3] F.C. Zhang, T.M. Rice, Phys. Rev. B **37**, 3759 (1988)

[4] P.W. Anderson, Phys. Rev. **86**, 694 (1952)

[5] A.L. Fetter and J.D. Walecka, *Quantum Theory of Many-Particle Systems* (McGraw-Hill, San Francisco, 1971)

[6] R. Coldea, S.M. Hayden, G. Aeppli, T.G. Perring, C.D. Frost, T.E. Mason, S.-W. Cheong, and Z. Fisk, Phys. Rev. Lett. **86**, 5377 (2001)

[7] L.N. Bulaevskii, E.L. Nagaev, and D.L. Khomskii, Sov. Phys. JETP. **27**, 836 (1968)

[8] S.A. Trugman, Phys. Rev. 37, 1597 (1988); *ibid* Phys. Rev. B **41**, 892 (1990)

[9] R. Eder and K.W. Becker, Z. Phys. B **78**, 219 (1990)

[10] S. LaRosa, I. Vobornik, F. Zwick, H. Berger, M. Grioni, G. Margaritondo, R.J. Kelley, M. Onellion, and A. Chubukov Phys. Rev. B **56**, R525(R) (1997)

[11] S. Sachdev and R.N. Bhatt, Phys. Rev. B **41**, 9323 (1990)

[12] S. Gopalan, T.M. Rice, and M. Sigrist, Phys. Rev. B **49**, 8901 (1994)

[13] B. Normand and Ch. Rüegg, Phys. Rev. B **83**, 054415 (2011)

[14] E. Dagotto and T.M. Rice, Science **27**, 618 (1996)

[15] H.B. Callen, *Thermodynamics and an Introduction to Thermostatistics* (Wiley, 1985)

[16] A.T. Savici, G.E. Granroth, C.L. Broholm, D.M. Pajerowski, C.M. Brown, D.R. Talham, M.W. Meisel, K.P. Schmidt, G.S. Uhrig, and S.E. Nagler, Phys. Rev. B, **80**, 094411 (2009)

[17] J.M. Tranquada, H. Woo, T.G. Perring, H. Goka, G.D. Gu, G. Xu, M. Fujita, and K. Yamada, Nature **429**, 534 (2004)

[18] R. Eder, Phys. Rev. B **100**, 085133 (2019)

[19] M. Fujita, H. Hiraka, M. Matsuda, M. Matsuura, J.M. Tranquada, S. Wakimoto, G. Xu, and K. Yamada, J. Phys. Soc. Jpn. **81**, 011007 (2012)

[20] L.D. Landau and E.M. Lifshitz: *Lehrbuch der Theoretischen Physik* (Akademie Verlag Berlin, 1988)